Print-on-Demand Facsimile of Online Articles

PALAIOS

Emphasizing the Impact of Life on Earth's History

July 2015 Volume 30, No. 7

An International Journal of SEPM
(Society for Sedimentary Geology)

PALAIOS
Emphasizing the impact of life on Earth's history

PALAIOS, 2015, v. 30, 553–573
Research Article
DOI: http://dx.doi.org/10.2110/palo.2014.064

SEDIMENTARY FACIES AND DEPOSITIONAL ENVIRONMENTS OF DIVERSE EARLY PALEOCENE FLORAS, NORTH-CENTRAL SAN JORGE BASIN, PATAGONIA, ARGENTINA

EMILY E. COMER,[1] RUDY L. SLINGERLAND,[1] J. MARCELO KRAUSE,[2] ARI IGLESIAS,[3] WILLIAM C. CLYDE,[4] MARÍA SOL RAIGEMBORN,[5] AND PETER WILF[1]

[1]*Department of Geosciences, Pennsylvania State University, University Park, Pennsylvania 16802, USA*
[2]*Museo Paleontológico Egidio Feruglio (CONICET-UNPSJB), 9100 Trelew, Argentina*
[3]*Universidad Nacional del Comahue, Instituto de Investigaciones en Biodiversidad y Ambiente INIBIOMA-CONICET, San Carlos de Bariloche 8400, Río Negro, Argentina*
[4]*Department of Earth Sciences, University of New Hampshire, 56 College Rd., Durham, New Hampshire 03824, USA*
[5]*Centro de Investigaciones Geológicas (CONICET-UNLP), Facultad de Ciencias Naturales y Museo, Universidad Nacional de La Plata, 1900 La Plata, Argentina*
e-mail: pwilf@psu.edu

ABSTRACT: **We here investigate the sedimentology of the early Danian (ca. 66–64 Ma) Salamanca Formation in the north-central San Jorge Basin, southern Chubut Province, Patagonia, Argentina, in order to place the outstandingly diverse and well-preserved fossil floras it contains into specific environmental settings. These assemblages are among very few of Danian age from the entire Southern Hemisphere and thus provide critical data about geographic variation in recovery from the end-Cretaceous extinction. Understanding the depositional context of the Salamanca floras is necessary for comparison with other assemblages and for interpreting their exceptional preservation. The Salamanca Formation was deposited above a widespread erosional sequence boundary (SB-1) resulting from a relative base level rise and widespread marine transgression during the early Danian (Chron C29n). In response to this increase in accommodation space, a broad, shallow estuary formed that most likely extended westward at least as far as the San Bernardo belt. A transgressive systems tract was deposited in this estuary, consisting of bioturbated sand fining upwards to silt. The maximum marine flooding surface at the beginning of the highstand systems tract is defined by well laminated, unburrowed, clay deposits of a low energy, deep shelf. The Salamanca highstand systems tract (HST) consists of sandy and silty facies capped by accreting subtidal bars and sandy shoals containing an abundance of tidal indicators, suggesting deposition proximal to the San Jorge paleo-estuary head. A second sequence boundary (SB-2), formed during Chron C28r and early C28n, separates the older highstand deposits from younger lowstand and transgressive deposits. These consist of estuarine sand shoals, trough cross-bedded sands deposited in aggrading, fluvially influenced tidal channels, tidal flat muds, and bayhead deltas. The best preservation of compression floras and petrified trees occurred near the tops of subtidal bars below SB-2; at the end of the shallowing-upward cycle that caps the second HST; and in fluvially-influenced tidal channels, tidal flat mudstones, and bayhead deltas of the lowstand and transgressive systems tracts that lie above SB-2. These settings were proximal to the source forests and had rapid rates of burial. We interpret the dark muds of the Banco Negro Inferior, which cap the Salamanca Formation, as a late transgressive and highstand systems tract deposited during a time of rising groundwater table and declining river slopes in a widespread, lowland coastal forest.**

INTRODUCTION

The Salamanca Formation of Chubut and Santa Cruz provinces, Patagonia, Argentina preserves exceptionally diverse and well-preserved compression floras, permineralized trunks and stumps, and microfloras from the early Paleocene (early Danian) that hold singular importance for understanding Southern Hemisphere paleobotany, paleoclimates, and paleo-landscapes in the wake of the end-Cretaceous extinction (Berry 1937; Romero 1968; Archangelsky 1973, 1976; Petriella and Archangelsky 1975; Archangelsky and Zamaloa 1986; Zamaloa and Andreis 1995; Matheos et al. 2001; Brea et al. 2005, 2007, 2008, 2011; Iglesias et al. 2007; Scafati et al. 2009; Clyde et al. 2014). Although previous workers agree on an epicontinental to coastal setting for these deposits, paleoenvironmental interpretations of the Salamanca Fm. are varied and sometimes contradictory. This paper presents a detailed interpretation of the depositional context of these rocks with the aim of answering two overarching questions: what landscapes supported such a diversity of plant species, and what local depositional conditions led to their superb preservation?

In the north-central San Jorge Basin of southern Chubut, several thousand macrofossil compression specimens, a vast increase from previous studies, have been recently documented in the Salamanca Fm. at three localities (Fig. 1): Palacio de los Loros (PL), Ormachea Park (Bosque Petrificado José Ormachea, OR), and Rancho Grande (RG) (Iglesias 2007; Iglesias et al. 2007). A fourth locality, Las Flores (LF) lies within the younger (late Danian) Peñas Coloradas Formation of the Río Chico Group (Fig. 2; Iglesias 2007; Clyde et al. 2014).

Taken together, macrofloras at these four sites provide an outstanding, well-dated (Clyde et al. 2014), and very rare record of plant diversification and biogeography in Gondwana shortly after the end-Cretaceous extinction. Several taxonomic occurrences are noteworthy (Iglesias et al. 2007), including the oldest evidence of legumes (*Paracacioxylon frenguellii* wood; Brea et al. 2008), and multiple organs of *Agathis*, a biogeographically significant araucarian conifer (Escapa et al. 2013). In

Published Online: July 2015
 0883-1351/15/030-553/$03.00

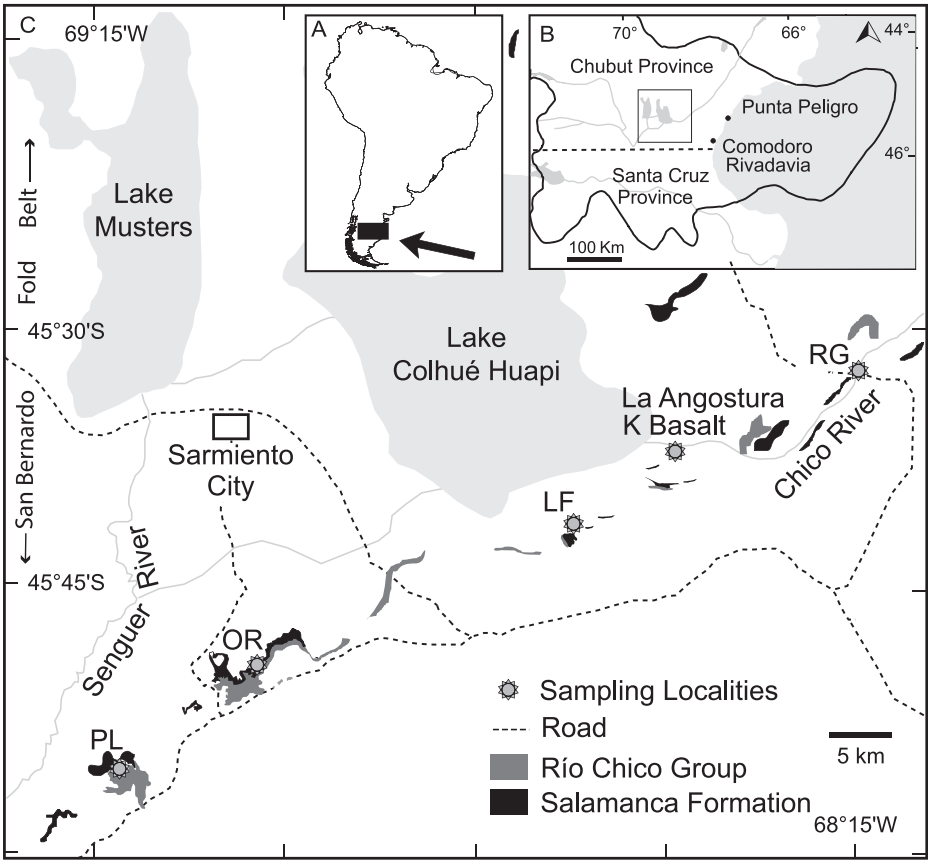

FIG. 1.—Map showing the San Jorge Basin and relevant localities (modified from Clyde et al. 2014). **A**) Location of study area. **B**) Boundary of the San Jorge Basin (solid line) as described by Sylwan (2001); gray represents lakes and rivers. **C**) Salamanca Fm. outcrops in black and Rio Chico Group in dark gray (Brea et al. 2005; Iglesias 2007). The dashed lines represent major highways 20 and 26 in the area. Sampling localities: PL = Palacio de los Loros; OR = Ormachea Park; LF = Las Flores; RG = Rancho Grande.

addition, the elevated floral richness found at PL contrasts sharply with the low diversity found in coeval northern hemisphere floras and suggests a relatively muted K–Pg floral extinction and faster recovery in Patagonia (Iglesias et al. 2007). This interpretation is corroborated by recent palynological work in northwest Chubut (Barreda et al. 2012) and, more broadly, by numerous cases of lineage survival in both plants and vertebrates (see Wilf et al. 2013).

Outside our study area, along the modern coast, the Salamanca Fm. preserves the important Peligran vertebrate faunas in its uppermost unit, known as the Banco Negro Inferior (BNI; Fig. 2). These have tremendous significance as the only well-dated, early Paleocene vertebrate assemblages from Gondwana (e.g., Pascual et al. 1992, 2002; Bonaparte et al. 1993; Bonaparte and Morales 1997; Gelfo and Pascual 2001; Bona 2007; Gelfo et al. 2007; Sterli and de la Fuente 2012; Clyde et al. 2014).

Understanding the depositional context of these exceptional fossil floras and faunas is critical for comparison with coeval fossil material from other parts of the world, in the context of recovery of terrestrial environments after the end-Cretaceous mass extinction. However, paleodepositional interpretations of the Salamanca Fm. are varied and sometimes contradictory. Feruglio (1949) first described the Salamanca Fm. as containing four members: Lignitífero, Glauconítico, Fragmentosa, and Banco Verde. Andreis et al. (1975) later subdivided the Salamanca into two members. His Bustamante Mbr. corresponds to basal, calcareous limestone beds that only crop out in the northeastern part of the San Jorge Basin, and his Hansen Mbr. includes all four units described by Feruglio as well as the Banco Negro Inferior. For the western exposures studied here, the most common classification of the Salamanca Fm. aligns with Feruglio's four members (Martínez 1992; Matheos et al. 2001 2005; Sylwan 2001; Iglesias 2007) capped by the Banco Negro Inferior. Opinions vary on whether the BNI should be included within the Salamanca Formation or the overlying Río Chico Group (e.g., Feruglio 1949; Andreis et al. 1975; Bonaparte et al. 1993; Foix et al. 2013; Fig. 2). Sedimentological evidence provided in this paper, along with paleomagnetic data (Clyde et al. 2014), places the BNI in a conformable sequence genetically related to the Salamanca; therefore, we include the BNI within the Salamanca Fm.

Martínez (1992) described four facies within the Salamanca Fm. in the area of this study: conglomerates, sandstones, claystones, and heterolithic facies. She interpreted a system of sand bars, delta lobes, tidal channels, and lagoons formed via slow marine transgression from the east, followed by a more rapid regression of a coast and inner shelf swept by tidal currents. Malumián and Caramés (1995) concluded from foraminiferal data that portions of the Salamanca Fm. were deposited under dysoxic conditions and low salinity. Bellosi et al. (2000) agreed with earlier workers that the lower Salamanca Fm. was produced during an Atlantic transgression. However, due to the presence of microfossils indicative of freshwater settings, they described the upper Salamanca Fm., including the BNI, as a wave-influenced tidal estuary that evolved into an extensive brackish lagoon. Matheos et al. (2001) described the Salamanca Fm. at Victor Szlápelis fossil forest, close to Palacio de los Loros, as containing

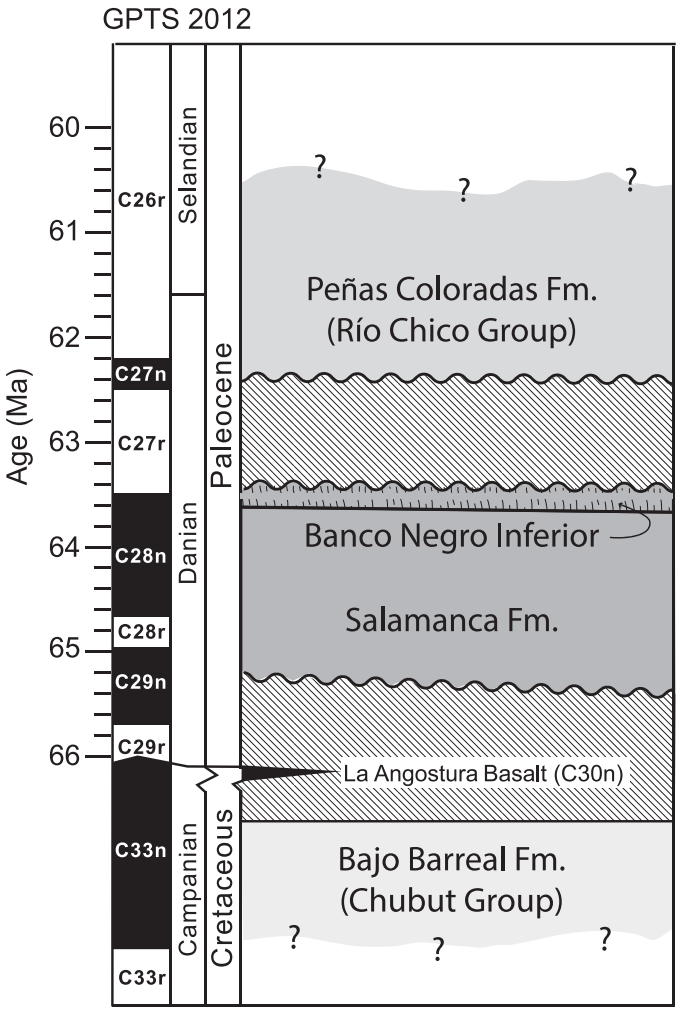

FIG. 2.—Generalized chronostratigraphy of latest Cretaceous and Paleocene geological units within the study area of the north-central San Jorge Basin, based on descriptions by Feruglio (1949), Uliana and Biddle (1988), Sylwan (2001), Raigemborn (2006), Iglesias (2007), Raigemborn et al. (2009), Krause and Piña (2012), and new age data in Clyde et al. (2014). Cross-hatch = section missing from non-deposition or erosion.

claystones, tuffaceous claystones, siltstones, and sandstones deposited in meandering fluvial and deltaic systems. Iglesias (2007) divided the Salamanca Fm. in its western exposures into a lower, middle, and upper member. His upper member contains well-preserved plant compression fossils in mudstones and fine-grained sandstones, thought to be deposited in channels and oxbow fills of a meandering, low-relief fluvial system (see also Iglesias et al. 2007). Most recently, Foix et al. (2012a) interpreted the Salamanca Fm. in the subsurface, using 3D seismic data on the Perales anticline, 50 km south of the study area. They defined a 600 km^2 deltaic system that prograded to the northeast and was fed by a 30 km long, east-west paleochannel. On this basis, they interpreted the Salamanca facies at Ormachea Park (Fig. 1) as comprised of distributary channel sands, river mouth bars, and interdistributary bay deposits.

This paper focuses on the sedimentology of the early Danian Salamanca Fm. in the north-central San Jorge Basin, near the city of Sarmiento in southern Chubut Province, Patagonia, Argentina. We describe 12 sedimentary facies from relatively continuous outcrops, along an oblique dip line in the proximal, westernmost exposures of the formation. We use facies geometries, paleocurrent data, and sandstone and mudstone mineralogy to define the sedimentary environments of deposition. We test a conjecture of a vigorous tidal estuarine environment by using an engineering hydrodynamic model to compute the paleotides expected in the San Jorge embayment. The result is a detailed paleogeographic and paleoenvironmental reconstruction of the study region during the early Danian. This reconstruction provides a significantly updated depositional framework for the Salamanca Fm. and refines the chronostratigraphy of Clyde et al. (2014), showing that the Salamanca macrofloras were preserved during both Chrons C29n and C28n.

GEOLOGIC SETTING AND STRATIGRAPHY

The Salamanca Fm. was deposited in the Golfo San Jorge Basin of central Patagonia, Argentina (Fig. 1), during the early Paleocene (early Danian; Clyde et al. 2014). The basin covers approximately 170,000 km^2 and is bordered on the north by the Somuncura Massif, to the south by the Deseado Massif and to the west by the Andean Cordillera; it continues eastward in the South Atlantic Ocean to the continental margin. The basin initiated due to Middle-Late Jurassic continental extension that caused the opening of the South Atlantic Ocean, the eventual separation of South America from Africa, and the creation of NNW-SSE- trending normal faults that formed large half-graben depocenters throughout Patagonia (Rodriguez and Littke 2001; Spalletti and Franzese 2007). The San Jorge Basin is divided into an eastern and a western component by the N-S trending San Bernardo fold belt just west of Lake Musters (Sylwan 2001; Fig. 1). Along the eastern flank of the San Bernardo fold belt lie the westernmost outcrops of the Salamanca Fm. Our study area encompasses these and more eastern outcrops in the north-central San Jorge Basin between present-day coordinates 45°–46° S and 68°–69° W, near the city of Sarmiento and the southern border of Chubut province (Fig. 1).

During the Campanian, the study area accumulated gray and red siltstones, mudstones, sandstones, and pyroclastic deposits of the upper Bajo Barreal and Laguna Palacios formations of the Chubut Group, interpreted to represent lakes and alluvial plains (Sylwan 2001; Iglesias 2007; Umazano et al. 2009; Fig. 2). These formations are truncated by a regional unconformity, immediately above which sit 500–1300 m (Sylwan 2001) of Cenozoic claystones, tuffs, and interbedded continental sandstones that alternate and intertongue eastward with shallow marine deposits. The oldest exposed strata in the Cenozoic sequence are assigned to the 30–200 m thick Salamanca Fm. Stratigraphically above the Salamanca Fm. lies the Peñas Coloradas Fm. of the Río Chico Group, a 50–250 m thick section of mudstones, sandstones, and conglomerates of terrestrial and mainly fluvial origin (Feruglio 1949; Sylwan 2001; Iglesias 2007; Raigemborn et al. 2009).

New chronostratigraphic results from the Salamanca and Peñas Coloradas formations in the Sarmiento area show that both are older than previously thought, being early and late Danian in age, respectively (Clyde et al. 2014). The new age estimates are constrained by (1) the unconformable stratigraphic position of the Salamanca Fm. above a re-dated, latest Cretaceous basalt (i.e., La Angostura basalt in Fig. 2); (2) preservation of early Danian foraminifera, calcareous nannoplankton, and dinoflagellates at the base of the Salamanca Fm.; (3) a re-dated, late Danian volcanic tuff in the Peñas Coloradas Formation; and (4) the measurement and correlation of the Salamanca Fm. magnetic polarity to Chrons C29n and C28n. Specifically, the rich macrofloras and permineralized trees in the upper Salamanca Fm. that are emphasized here correlate to C29n, or 65.58–64.86 Ma, and C28n, or 64.67–63.49 Ma on the 2012 Geomagnetic Polarity Timescale (GPTS; Gradstein et al. 2012). Farther east and near the coast, the Salamanca Fm. has been estimated to be middle to late Danian in age based on foraminifera and ostracods, suggesting it is time-transgressive from west to east (Méndez

1966; Bertels 1975; Clyde et al. 2014) as also implied by reversed polarity in the BNI in that area (Marshall et al. 1997).

STUDY AREA

We studied four fossil localities in Chubut Province, Patagonia, Argentina (all coordinates in UTM WGS84, Zone 19 S; Fig. 1): Ormachea Park (OR; 495,000 m E, 4,925,300 m S), Palacio de los Loros (PL; 483,532 m E, 4,915,686 m S), Rancho Grande (RG; 559,059 m E, 4,956,123 m S), and Las Flores (LF; 529,660 m E, 4,940,152 m S). These localities contain 10 macrofossil sites: OR-1, OR-2, Cerro Solitario, PL-1, PL-2, PL-3, PL-4, PL-5, RG, and LF (Figs. 1, 2; also see Clyde et al. 2014). This study primarily focuses on Ormachea Park and Palacio de los Loros because these sites contain the largest numbers of individual fossil localities and expose the entire Salamanca Fm. In particular, two quarry sites at Palacio de los Loros (PL-1 and PL-2) provided the quantitative paleobotanical data that showed elevated floral richness after the K–Pg extinction (Iglesias et al. 2007), and among these, quarry PL-2 superbly preserves flowers, fruits, seeds, and leaves with cuticles, as well as other delicate fossils such as insect wings and feathers (Tambussi and Degrange 2013). The stratigraphically isolated plant localities at RG and LF are evaluated here briefly. The RG locality occurs in a significantly different facies of the Salamanca Fm. that indicates a deeper-water environment, and the LF locality occurs within the basal strata of the younger Peñas Coloradas Fm. of the Río Chico Group (Iglesias 2007; Clyde et al. 2014).

METHODS

Data analyzed here came from two field seasons, during February-March 2010 and April-May 2011. At OR and PL, where exposures are good to excellent, stratigraphic columns were measured on multiple cliff faces and through all the main plant localities. Sandstone composition, grain size, and grain roundness were estimated by hand lens in the field and verified by point counting of thin sections. Samples were stained for plagioclase and potassium feldspar and point-counted using an Olympus petrographic microscope. Three hundred points per sample were counted using the Gazzi-Dickinson method (Dickinson and Suczek 1979), and grains were divided into sixteen categories following the classification of Folk et al. (1970). Analysis of grain size was performed using Gradistat version 6.0 (Blott and Pye 2001).

Nineteen samples were collected from the upper 12 m of the Salamanca Fm. at OR for a clay mineralogy study (Fig. 3). These samples were ground to a uniform 4 μm fraction and x-rayed as an unaltered powder sample, as an oriented powder sample on a glass mount, as an oriented powder sample on glass mount exposed to ethylene glycol for 24–48 hours to ensure clay expansion, and as an oriented sample on a glass mount heated to 550° C for 2 hours to ensure mineral collapse. The USGS Clay Mineral Identification Flow Diagram (Poppe et al. 2001) was used to determine the clay minerals. A full chemical analysis of the oxides in these sediments was performed using a Perkin-Elmer Optima 5300 ICP (inductively coupled plasma spectrometer), after dissolution of the ground sediments by lithium metaborate.

Total organic-carbon (TOC) content of each paleosol and rock sample was obtained by elemental analysis of decarbonated sample aliquots. Fifty grams of ground and sieved material were reacted with 1N HCl for 30 minutes, neutralized thoroughly with deionized water, and then lyophilized for 48 hours before analysis. Organic carbon was measured by combustion in a Costech EA coupled to a Delta XP mass spectrometer via a Conflo system. Evolved gases were dried, then oxidized by chromium oxide and cobalt oxide, and reduced by elemental copper. Simultaneous analysis of internal and IAEA standards along with reference gases results in precision and accuracy approaching 0.3%.

Paleocurrent data on the large-scale trough and planar cross-strata formed by dunes were measured on slip faces by excavating the weakly consolidated sandstones to expose a three-dimensional bedding plane. The resulting circular histograms were tested for uniformity using the azimuth statistic, U^2 (Jones 2006) given by:

$$U^2 = \sum_{i=1}^{N} \left[U_i - \overline{U} - \frac{i-1/2}{N} + \frac{1}{2} \right]^2 + \frac{1}{12N} \quad (1)$$

where U_i are the observed azimuthal data, $\overline{U}$ is their simple mean, and N is the number of observations. U^2 measures the sum of the deviations of cross-strata dip azimuths from a theoretical uniform circular distribution.

FACIES DESCRIPTIONS

The investigated strata (Figs. 1, 4) can be subdivided into 12 facies (Table 1; Fig. 5), here organized from coarsest- to finest-grained (size classification according to Farrell et al. 2012).

Facies S_{wc}*: White Cross-Bedded Sandstones*

Description.—Facies S_{wc} consists of moderately sorted (fL-cU), poorly cemented, white litharenite (Fig. 5A–E, G). The grain size distribution is unimodal, with a sample median grain size of 704 μm, corresponding to cL sand. Quartz grains are angular to sub-angular. Facies S_{wc} contains the highest quartz fraction of any collected sample, with 60% quartz, 10% feldspar, and 30% lithic grains. Sedimentary structures include trough cross-beds in bedsets ranging from 0.5–3 m in thickness, progressive thickening and thinning of cross-beds in individual sets symptomatic of spring-neap tidal bundles, and occasional convolute bedding. The top of this facies often contains mud drapes (Fig. 5C). Paleocurrent data taken from cross-beds indicate polymodal current directions (Fig. 6). According to the U^2 statistic, the orientation data are not uniformly distributed at the 95% confidence interval but cluster in the NW and SW quadrants, suggesting bi-directional flows. Permineralized logs and tree stumps (Fig. 5E) protrude from cliff faces and litter the landscape underlain by this facies. The roots and wood of logs and stumps are abraded. Compressed plant fossils occur below the base of this facies as well as above its upper contact.

Facies S_{wc} is variable in thickness, ranging from 3 to 24 m. It always lies unconformably over facies S_{hc}, and its upper contact is transitional, usually interfingering with the overlying fine-grained facies S_{ab} (Fig. 5B). Facies S_{wc} is present at PL and OR exposures, and along cliff faces in between.

Interpretation.—Facies S_{wc} is the equivalent of the Banco Verde member described by Feruglio (1949). Consistent with Martínez (1992) and Matheos et al. (2001), we interpret this facies as elongate sand bars deposited in open marine environments and in tidal channels near the headwaters of a tide-dominated estuary (Dalrymple et al. 1990). Typical flow velocities transporting and depositing facies S_{wc} must have ranged from 0 to 1.5 m s^{-1}, as estimated from its coarse grain size, large-scale dunes, and its abundance of permineralized logs and stumps (Fig. 5E). Water depth in the tidal channels can be estimated from dune height by assuming that approximately one-third of the dune slip-face is preserved in cross-strata (Leclair 2002) and that dune height is approximately one-fifth of water depth (Leeder 2011). Average cross-bed thickness in this facies ranges from 1/4 to 2 m, thereby corresponding to a total dune height of 3–6 m and water depths of 3–30 m. Paleocurrent directions are strongly bimodal in facies S_{wc}, and, when combined with cross-bed mud drapes and spring-neap cross-strata thickening and thinning, provide significant evidence for vigorous tidal currents.

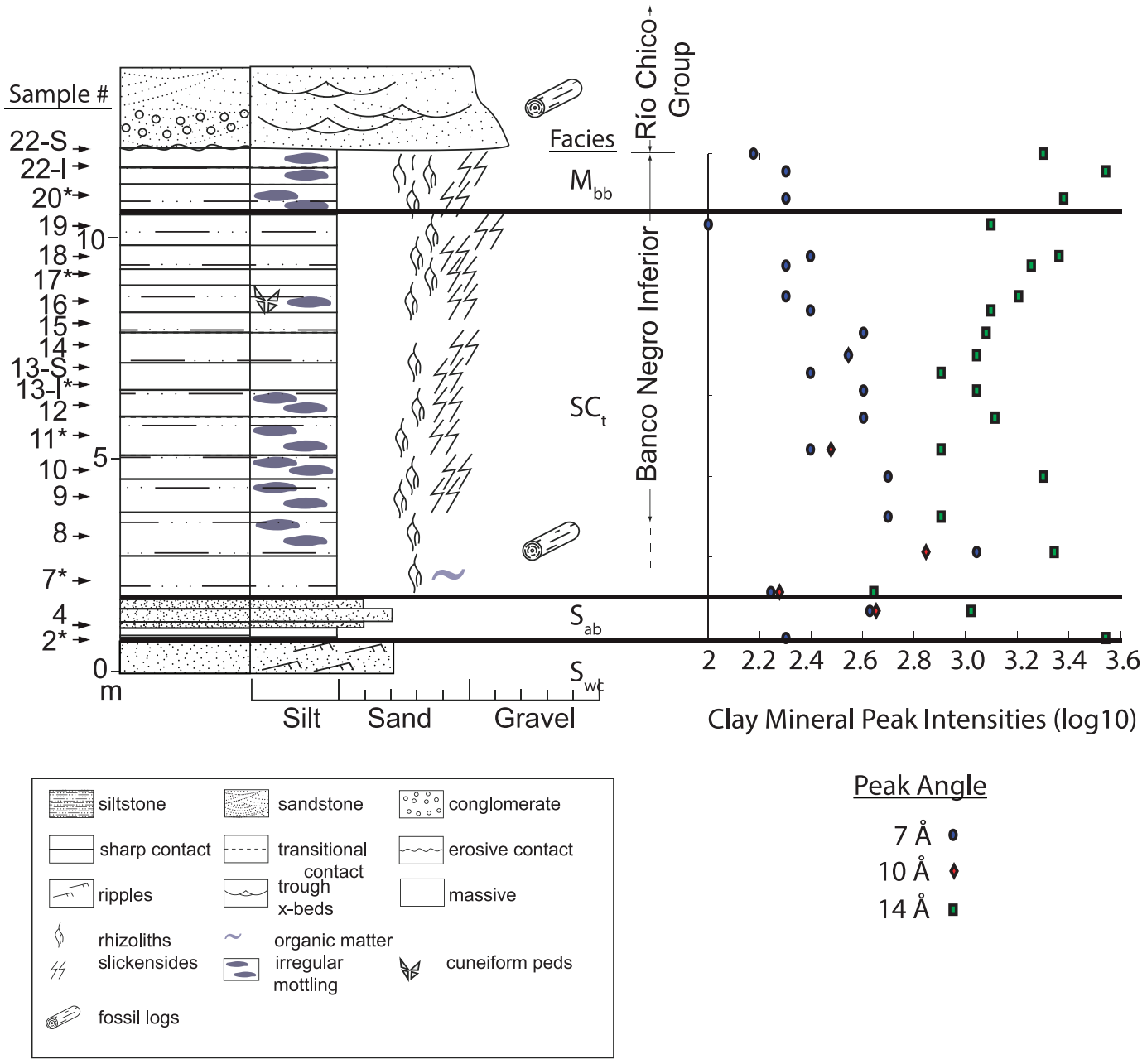

FIG. 3.—Graphic log from cliff face adjacent to plant locality OR-1 (denoted by star in locality inset map of Figure 4A), showing stratigraphic locations of XRD and chemical analysis samples. Samples used in the chemical analyses are 2, 7, 11, 13-I, 17, and 20 (denoted by asterisks). Facies definitions summarized in Table 1. Clay mineral peaks are interpreted as: 7 Å = a kaolin-mineral; 10 Å = illite/glauconite; and 14 Å= smectite. Intensity of the 7 Å peak shows a general decline upwards.

Mud drapes in upper portions of facies S_{wc} indicate a vertical decrease of flow strength, as might be expected on tidal bars adjacent to a tidal channel. Interfingering at the upper contact of facies S_{wc} and facies S_{ab} indicates that both facies were deposited simultaneously, in adjacent depositional environments. Both upright and overturned permineralized stumps occur within facies S_{wc} with abraded rootwads. The absence of extensive roots and paleosols beneath them are evidence that the stumps floated to their final resting places on estuarine tidal bars, as did the far more numerous fossil trunk segments. Their most likely origin is bank collapse upriver, similar to modern forested coastal environments.

Facies S_{uc}*: Unidirectional Cross-Bedded Sandstones*

Description.—Facies S_{uc} is a moderately sorted, poorly cemented tan-white litharenite composed of vcU angular grains and 30% lithics (estimated by hand lens). Facies S_{uc} is only found at one locality of PL, lying conformably within facies S_{wc} (Figs. 4C, 5D). It is comprised of a ~ 3 m thick solitary bedset of unidirectional, south-dipping (185°), high angle cross-strata that extends for more than a km along outcrop. The bedset contains occasional superimposed smaller-scale cross-strata dipping southwest.

Interpretation.—Facies S_{uc}, along with facies S_{wc}, is considered equivalent to the Banco Verde member described by Feruglio (1949).

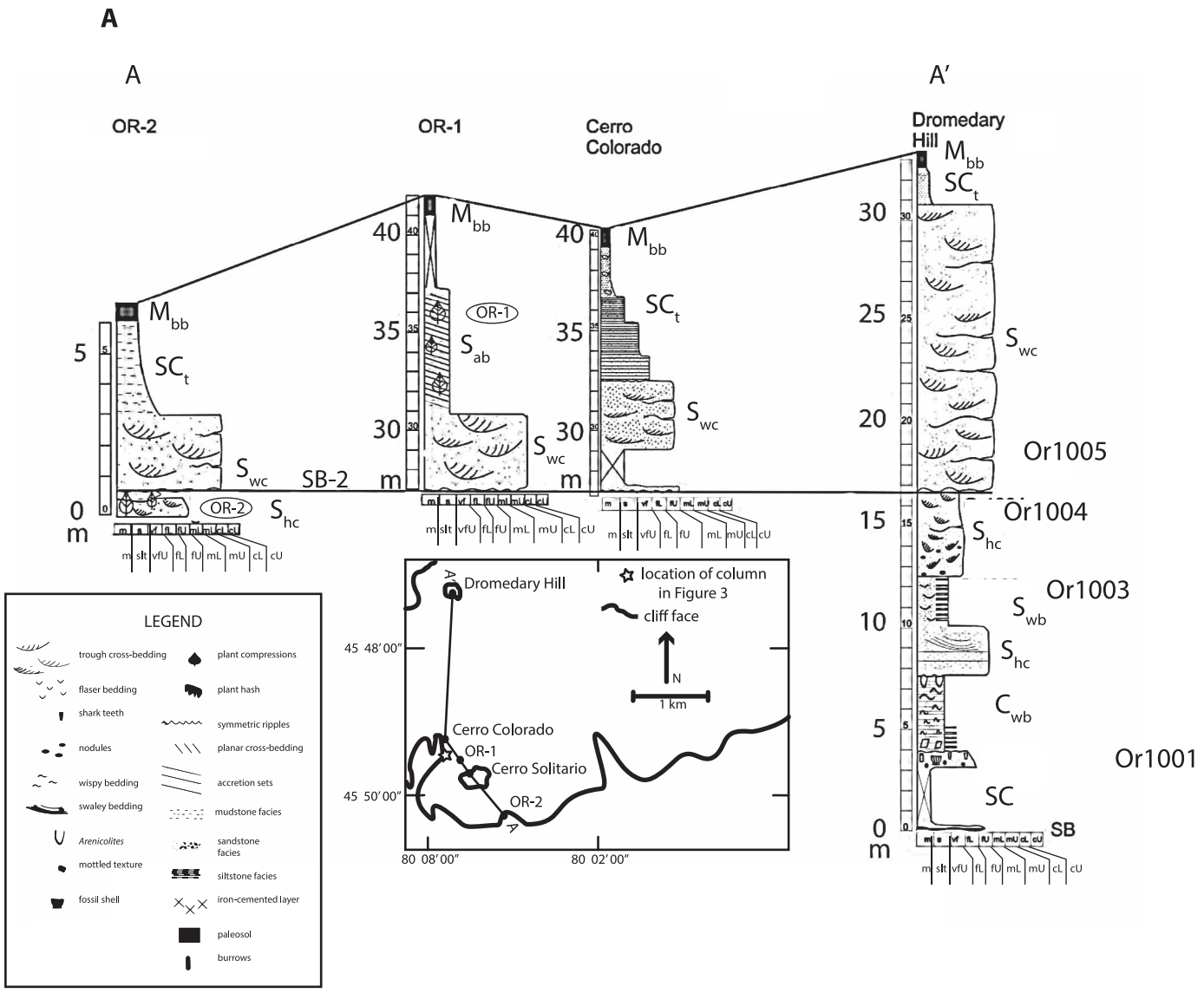

FIG. 4.—Selected graphic logs. **A**) Ormachea Park. **B**) Palacio de los Loros. Datum is an erosion surface defined as a sequence boundary (SB-2). Annotations refer to facies types in Table 1; OR1001 to OR1005 represent locations of samples for sand petrography; ellipses OR-1, PL-1, etc. denote macrofloral fossiliferous horizons.

Based on the thickness of the solitary bedset and the nature of associated cross-beds, this facies is interpreted to be either a runoff microdelta, created by late ebb currents during the transition to low tide (see, for example, Dalrymple et al. 1990), or a bayhead delta (Boyd et al. 1992).

Facies S_{ppl}*: Plane-Parallel Laminated Sandstones*

Description.—Facies S_{ppl} is a very poorly sorted, cL white litharenite composed of 30% lithics (observed by hand lens) with angular quartz grains (Fig. 5F). This facies displays low angle plane-parallel laminations, usually dipping west in bed sets of 10–20 cm. Steeply dipping, unidirectional cross-strata in 1–3 cm thick beds occasionally occur within these bed sets. Average thickness is approximately 2 m. Where observed, the lower contact of S_{ppl} is an erosional unconformity (note truncation in Fig. 5F), and its upper contact is sharp and defines the base of facies S_{ab}. Facies S_{ppl} is only seen at Ormachea Park.

Interpretation.—S_{ppl} is interpreted as sand flats deposited under an upper plane-bed flow regime. This facies lies at the same stratigraphic horizon as facies S_{wc} and replaces it laterally. The association with facies S_{wc} and the high flow velocities necessary to create plane-parallel laminations are typical of upper flow regime sand flats just seaward of the tide-dominated fluvial reach of an estuary where tidal energy reaches a maximum (Dalrymple et al. 1992).

Facies S_{hc}*: Heterolithic Cross-Bedded Sandstones*

Description.—S_{hc} is a moderately sorted, moderately to well-cemented litharenite consisting of 91% framework grains (Fig. 5G). The grain size distribution is bimodal, with a median grain size of 156 μm corresponding to fL sand. The sand composition consists of 43% quartz, 13% feldspar, and 44% lithic grains. Glauconite, grouped with the lithics, is abundant and comprises almost 11% of the entire mineral assemblage. Total organic carbon (TOC) values in S_{hc} range from 0.1–0.17%. S_{hc} is trough cross-stratified in 10–20 cm thick bi-directional bedsets, with sparse mudstone interbeds 1–2 cm thick. It lies unconformably below facies S_{wc}, in thicknesses ranging from 4–12 m. It contains plant debris and 0.5–1 cm mud rip-up clasts, and where observed it is bounded below by a sharp

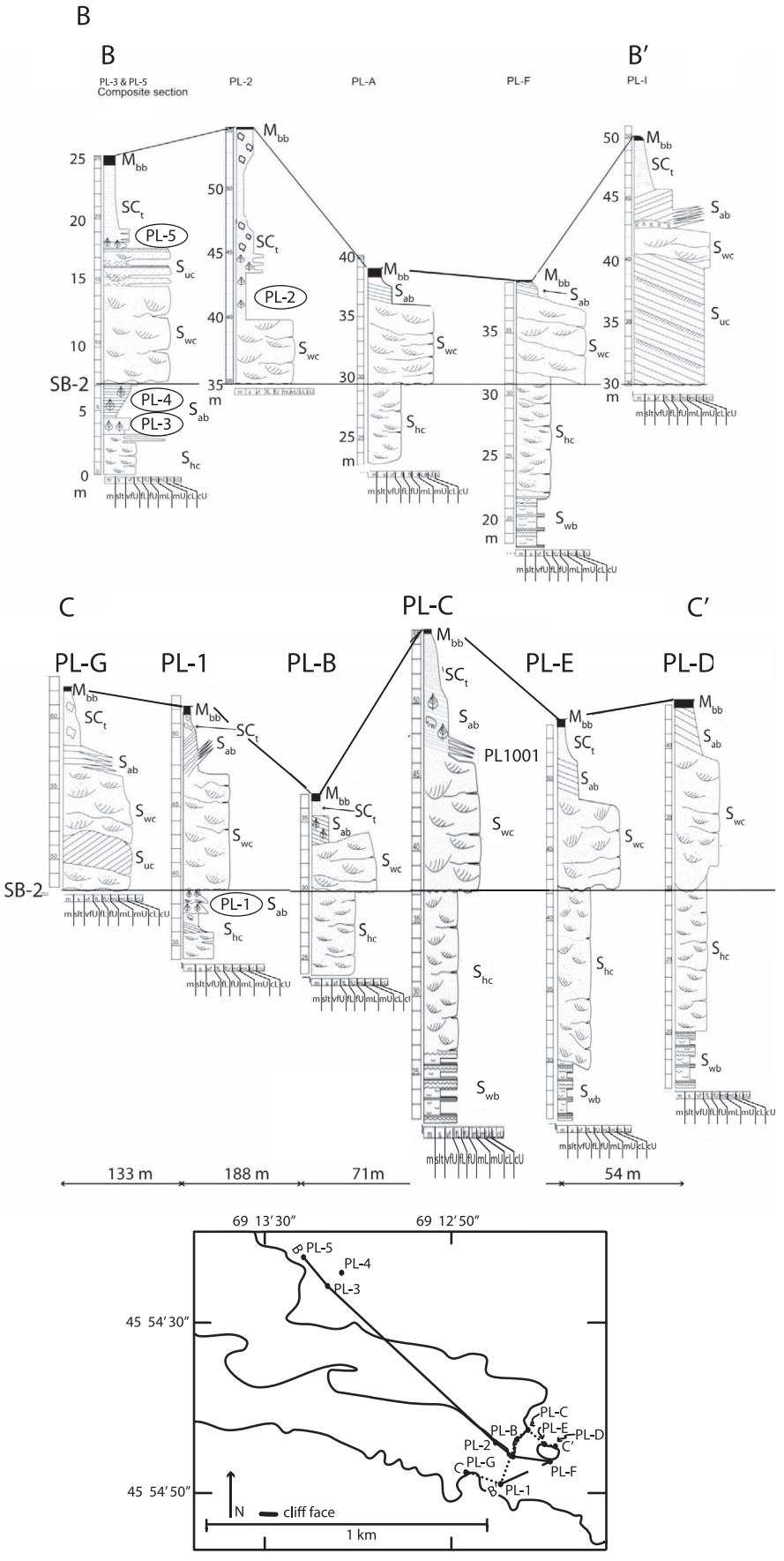

FIG. 4.—*Continued.*

TABLE 1.—*Summary of sedimentary facies and paleoenvironmental interpretations.*

Facies	Lithology and sedimentary structures	Fossil material	Interpretation
S_{wc}: White cross-bedded sands	Moderately sorted (fL-cU), poorly cemented, white litharenite containing meter-scale, multidirectional trough cross-bed sets		Sand bars deposited in deep tidal channels
S_{uc}: Unidirectional cross-bedded sands	Moderately sorted, poorly cemented, tan-white litharenite containing meter-scale, high angle, unidirectional cross-bed sets with occasional, superimposed cm-scale cross-strata		Runoff microdelta
S_{ppl}: Plane-parallel laminated sands	Very poorly sorted, cL white litharenite containing centimeter-scale low angle plane-parallel laminations		Sandflats near the estuarine headwaters
S_{hc}: Heterolithic cross-bedded sands	Moderately sorted, moderately to well-cemented glauconite-rich litharenite containing centimeter-scale trough cross-bed sets	Plant debris	Subtidal bars on a sand shoal that contains mutually evasive tidal channels
S_{shc}: Swaley-hummocky cross-bedded sands	fU, poorly sorted (vfU-mL), poorly cemented litharenite containing meter-scale swaley and hummocky cross-bedding		Storm deposits within tidal bars and channels
LF1: Poorly sorted, unidirectional cross-bedded sandstones	poorly sorted (fL-vC), poorly cemented white litharenite containing bedsets of unidirectional-dipping cross strata with occasional mud balls	Poorly preserved leaf fossils	Channel-fill
SC: Poorly sorted litharenites and clays	Alternating meter-scale sand and shale bodies. Sands are poorly sorted (fL-cU), poorly to moderately quartz-cemented litharenite	Sand filled burrows, shark teeth, plant debris	Transgressive lag deposit above a marine flooding surface
S_{wb}: Wavy-bedded sands and silts	Alternating sand-silt beds ranging in thickness from 1–5 cm containing wavy bedding and wave ripple cross-beds.	Plant debris	Deeper water deposits of a tidal estuary near the seaward limit of tidally influenced sediments
S_{ab}: Accretion-bedded sands and silts	Moderately well sorted homogeneous sands and silts consisting of centimeter-scale heterolithic inclined cross-bed sets	Well preserved plant remains	Lateral accretions beds of abandoned tidal channel fill
SC_t: Transitional sands to silty clays	Poorly to moderately cemented lithic wacke interbedded with silty clay containing fine laminations that grade into a mottled texture.	Well preserved plant fossils and plant debris	Tidal flats on a prograding lower coastal plain
C_{wb}: Wispy-bedded clays	Finely laminated purplish gray clay interbedded with centimeter-scale sand wisps	U-shaped burrows	Low energy, possibly anoxic, deepwater deposits
M_{bb}: Brownish black muds	Brownish black mud with pedogenic slickensides and iron nodules	Rhizoliths, plant fossils, mammals, and amphibians (Marshall et al. 1997)	Slowly prograding, widespread coastal-plain swamp experiencing a low rate of sediment supply

contact. S_{hc} is occasionally succeeded by accretion sets and laminated silts of facies S_{ab} and SC_t. S_{hc} occurs at OR, PL, and RG. At RG, the sand is a lithic wacke rather than a lithic arenite, and instead of trough cross-bedding it contains low angle cross-strata in bedsets of 10 cm with occasional clay rich laminations. It is the facies that preserves macrofloras from OR-2 and Cerro Solitario in Ormachea Park (Fig. 4A; Iglesias 2007).

Interpretation.—S_{hc} is interpreted as deposits of subtidal bars on a sand shoal. Tidal flows are a likely cause of the bi-directional trough cross-beds, mud drapes within cross-bed foresets, and heterolithic facies. The origin of the glauconite is problematic in that glaucony facies are representative of open marine environments experiencing low sedimentation rates within depths of 60–550 m (Odin and Fullagar 1988). Possibly, these glauconite minerals were eroded from deposits exposed on land or from scour of deeper water facies by subtidal channels. Plant debris within this facies was preserved in a siltstone lens likely deposited during a period of low energy slack water. This plant debris is comminuted and is interpreted to have been transported a long distance.

Facies S_{shc}*: Swaley-Hummocky Cross-Bedded Sandstones*

Description.—Facies S_{shc} (Fig. 4A, 5F; Dromedary Hill site at OR) consists of a fU, poorly sorted (vfU-mL), poorly cemented litharenite. Its grains are sub-angular. It exhibits large-scale swaley and hummocky cross-bedding in bedsets of 0.5–1 m. Facies S_{shc} is highly variable in thickness, ranging from 2.4–9.4 m over a few meters laterally in the Dromedary Hill section. It was only documented in two areas within OR and, where present, interfingers with S_{hc} and S_{wb}.

Interpretation.—Facies S_{shc} is interpreted as storm deposits within tidal bars and channels. Hummocky and swaley beds are only known to form under strong, combined directional and oscillatory flows, indicating that this facies was formed in water depths above storm wave base. The facies is anomalously coarse and poorly sorted for typical swaley bedforms, although Shieber (1988) reported swales and hummocks in medium-grained sandstone. Facies S_{shc} mirrors the composition of the facies with which it interfingers and is therefore interpreted to have formed in the same system of tidal bars and tidal channels that created S_{hc} and S_{wb}, possibly on their seaward side in deeper water, open to wind and waves.

Facies LF1*: Poorly Sorted Unidirectional Cross-Bedded Sandstones*

The younger (ca. 62 Ma) Peñas Coloradas Formation consists of only one facies in the small area of the Las Flores section visited in this study.

Description.—Facies *LF1* is a poorly sorted (fL-vC), poorly cemented white litharenite composed of 4–17% quartz, 18–28% feldspar, and 63–69% lithics. Grains are angular. This facies is comprised of 20–30 cm bedsets of unidirectional dipping cross strata with occasional mud balls

up to 5 cm, and a bed of reddish fissile mud wedged between crossbed sets. It is in this mud that leaf fossils are observed.

Interpretation.—We tentatively interpret this facies as a channel fill based on its poorly sorted, angular grains, mudballs, heterolithic cross-strata, and general stratigraphic context. Petrographic work (below) shows that this sand is not part of the Salamanca Fm. but has a strong volcanic signature that allows us to identify it as part of the Peñas Coloradas Fm.

Facies SC*: Poorly Sorted Litharenites and Clay Shales*

Description.—Facies *SC* (Fig. 5H) is a poorly sorted (fL-cU), poorly to moderately quartz-cemented litharenite–lithic wacke with a median grain size of 272 μm, corresponding to mL sand, although the grain size distribution is polymodal. In places, facies *SC* contains scattered pebbles. At OR, framework grains make up 93% of the sand beds and consist of 52% quartz, 12% feldspar, and 36% lithic fragments. The quartz grains are dominantly subangular. TOC values in this facies are ≤ 0.1%.

Sandstone beds of facies *SC* occur as tabular bodies about 30–100 cm thick that are bounded on their tops by sharp erosive surfaces and bounded at the top and base by 0.5–2 m clay intervals. The lowest occurrences of this facies usually contain cross-strata dipping at angles of 15–25°, whereas succeeding sand bodies are massive. Individual cross beds are 0.5–1 cm thick within 10– 20 cm thick bedsets. These sandstones contain phosphatic nodules, plant debris within mud drapes, shark teeth, shelly marine fossils, and 1–3 cm clay rip-up clasts. Some units also contain 0.5–2 cm wide, white, sand-filled burrows from the *Glossifungites* ichnofacies. The burrows are vertical to sub-vertical, sharp-walled and passively in-filled, and dominated by the ichnogenera *Diplocraterion* and *Skolithos*. A sample from facies *SC* also contained a pollen association dominated by *Classopollis*, of the extinct conifer family Cheirolepidiaceae, and green freshwater algal spores of the Zygnemataceae family (Clyde et al. 2014). Facies *SC* occurs at OR and RG, and at OR it comprises the first 4 m of the Salamanca Fm., directly above its unconformity with Late Cretaceous sediments.

Interpretation.—Facies *SC* is interpreted as the remains of a transgressive lag above a marine flooding surface. The multiple sandstone bodies interrupted by clay shale intervals are interpreted as a transgressive systems tract produced by the retrogradation of the shoreline and shoreface. Alternations between clay and sand beds are common in tide-dominated estuaries where partial transgressions are preserved seaward of a highstand shoreline (Dalrymple et al. 1990). Tidal influence is evident in the mud drapes on cross-bed foresets, and a marine origin is indicated by a diverse, shelly, marine-fossil fauna. The phosphatic nodules and trace fossils attributed to the *Glossifungites* ichnofacies also suggest a period of low sediment deposition rates, as expected in the later stages of a transgression and as noted by Mastandrea et al. (1983) in the eastern San Jorge Basin. Also present in this facies are microfossils such as Zygnemataceae algae spores, indicative of stagnant freshwater lakes or ponds (Bellosi et al. 2000; Matheos et al. 2005; Clyde et al. 2014). The spores and pollen are presumably allochthonous, transported from more proximal areas.

Facies S_{wb}*: Wavy-Bedded Sandstones and Siltstones*

Description.—Facies S_{wb} (Fig. 5I) consists of alternating sandstone-siltstone beds ranging in thickness from 5–11 cm, composed of grain sizes from vf sand to silt. The thickness of this facies ranges from 2–4 m. The sandstone beds are moderately sorted, poorly cemented, and composed of 49% framework grains and 51% silt-sized matrix grains, the latter having a unimodal grain size distribution with a median grain size of 59 μm. The mineral assemblage of the sandstone within this facies at OR is 48% quartz, 39% lithics (10% glauconite), and 13% feldspars. Some intervals are wavy-bedded, with 1–2.5 cm thick silt layers intercalated with 1–5 cm thick sandy siltstone beds. At some localities, these wavy bedsets alternate with wave-ripple cross-laminated bedsets as well as flaser and lenticular bedsets. Wave ripple lamination bedset thicknesses average 10–30 cm, but they thicken and thin systematically upwards as their grain size coarsens and fines. Some localities display convolute bedding, and some have 50–80 cm thick siltstone beds. At RG, facies S_{wb} contains a 40 cm thick coquina bed as well as 20–40 cm thick and 1–2 m long sandstone lenses. Everywhere observed, the facies contains abundant plant debris, and glauconite increases up-section. Facies S_{wb} usually underlies S_{hc} and occurs at OR, PL, and RG. Plant locality RG lies within Facies S_{wb} and contains macrofloras, brittle stars, and marine bivalves. A single large benthic foraminifer was recovered from this facies at RG (Clyde et al. 2014).

Interpretation.—This facies is representative of shelf deposits of a tidal estuary (Zhang and Zhang 2008). Flaser, wavy, and lenticular bedding are also common in tidal flat settings, but tidal flat laminations are commonly thinner and muddier and are only preserved in intertidal zones (Dalrymple et al. 1990; Choi et al. 2004). The rhythmic alternations in facies S_{wb} are evidence of a tidal setting, with coarser-grained beds deposited during tidal flows and fine-grained beds deposited during slack-water. Thinner beds represent neap tides, and thicker beds represent spring tides (Shanmugam et al. 2000). High glauconite content and wave-rippled laminations imply a strong marine influence; thus, these facies probably lie near the seaward limit of tidally influenced sediments. The large benthic foraminfer found at RG signifies an inner to middle shelf environment (Clyde et al. 2014), and its good preservation suggests autochthonous fossilization. The inferred environment of facies S_{wb} is an inner to middle shelf environment at the limit of tidally influenced sediments. The preserved macroflora at RG was thus transported farther than the river-influenced estuarine macrofloras at PL and OR.

Facies S_{ab}*: Accretion-Bedded Sandstones and Siltstones*

Description.—Facies S_{ab} (Fig. 5B, D, F, G) consists of thin heterolithic inclined strata unidirectionally dipping 10–15°, and it is composed of moderately well sorted, homogeneous sandstone and mudstone beds. The sandstones are comprised of a bimodal distribution of grain sizes whose median size is 85 μm, corresponding to vfL sand. Framework grains make up 85% of the sediment and are composed of 42% sub-rounded quartz, 10% feldspar, and 48% lithic grains; TOC values in this facies are less than 0.1%. The total thickness of this facies at any one locality lies between 0.5–3 m. The base of facies S_{ab} generally interfingers with various underlying facies, and the upper contact is transitional. This facies occurs in two stratigraphic positions—above facies S_{wc} at PL and OR, and above S_{hc} at PL. Well-preserved leaf-compression fossils (fossil localities OR-1, PL-1, PL-2, and PL-4) are found within and above this facies.

Interpretation.—Inclined heterolithic cross-strata are commonly described as lateral accretion beds of point bars, and this is how we interpret facies S_{ab} (Nouidar and Chellai 2001; Crerar and Arnott 2007). The occurrence of facies S_{ab} above facies S_{wc} (Fig. 5B) defines a shallowing-upward sequence from subtidal channel deposits to intertidal point-bar accretion beds. Based on the interbedded fine sand and mud component, this facies is interpreted as tidal channel fill deposited during channel migration and progressive abandonment (Willis and Tang 2010). Because facies S_{ab} is less than 5 m thick, displays unidirectional dips within one succession, and lacks internal erosional surfaces, it is thought to represent deposits of single point bars, as opposed to amalgamated deposits. From the thickness of the point bar, channel width w can be roughly estimated based on the equation:

$$w = 6.8h^{1.54} \quad (2)$$

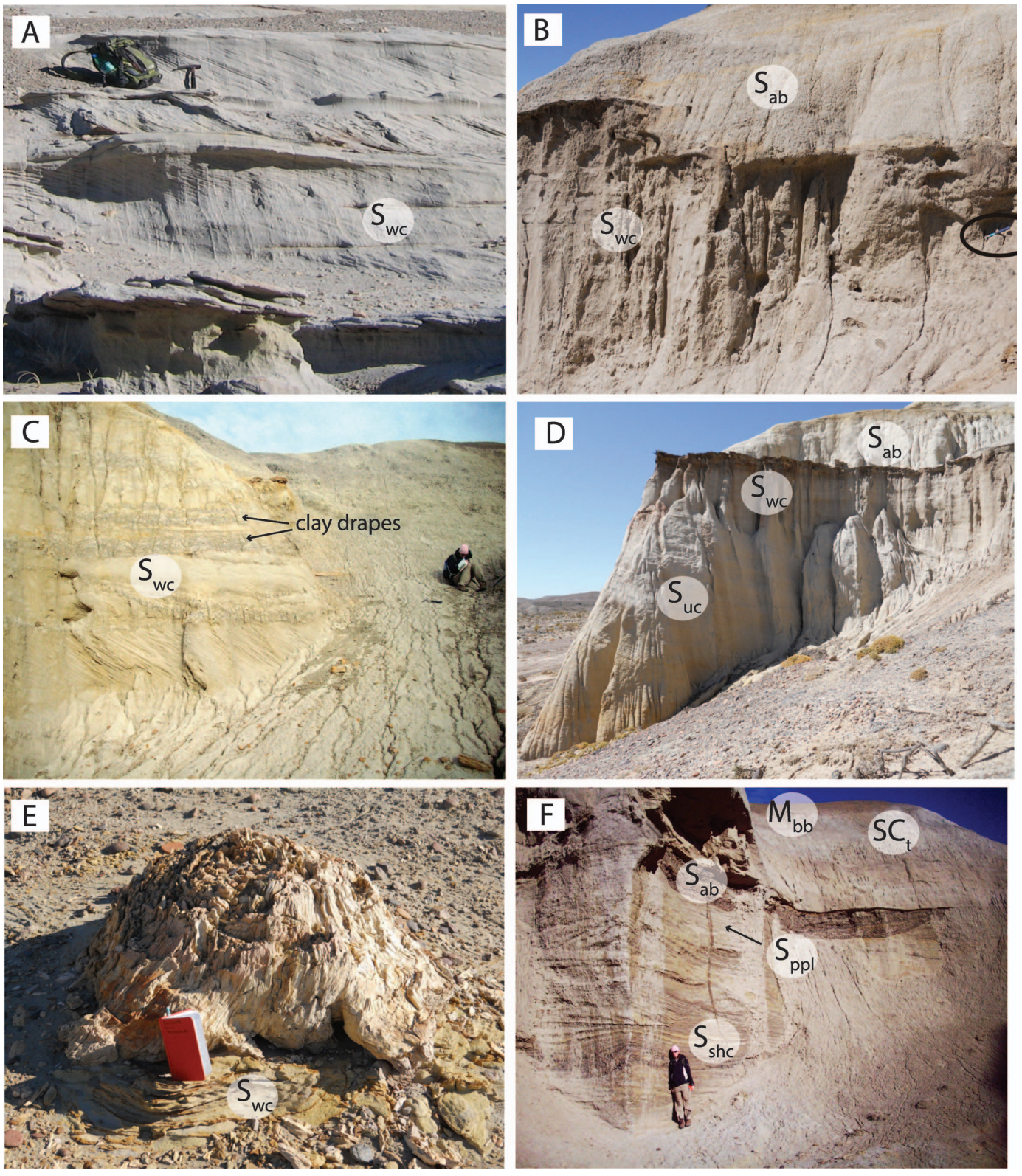

FIG. 5.—Field photos showing facies described in text. **A**) Facies S_{wc} (white cross-bedded sandstone) from OR. **B**) Facies S_{wc} interfingering with facies S_{ab} (accretion-bedded siltstone) at PL (hammer circled for scale). **C**) Mud drapes and lenticular rhythmic bedding within facies S_{wc} at PL. **D**) Facies S_{uc}—solitary set of planar cross-strata from PL lying conformably within facies S_{wc}–white trough cross-bedded sandstone. **E**) Permineralized stump from OR. **F**) Facies S_{shc} (swaley-hummocky cross-bedded sandstone) unconformably capped by S_{ab} (accretion-bedded sandstone and siltstone) and overlain by SC_t, and M_{bb} (finer silty sandstone grading into black mudstone of the BNI) at OR. **G**) Progression of facies S_{wb} (flaser, wavy, and lenticular rhythmic bedding), S_{hc} (heterolithic sandstone), S_{wc}, S_{ab}, SC_t, and M_{bb} (black mudstone of the BNI) at PL. **H**) Facies *SC* (poorly sorted litharenites and clay balls) at OR. **I**) facies S_{wb} at Abigarrado Hill, OR. **J**) PL-2 locality and plant fossils from facies SC_t. **K**) Facies C_{wb}–wispy bedded clay shale with burrows near its upper contact.

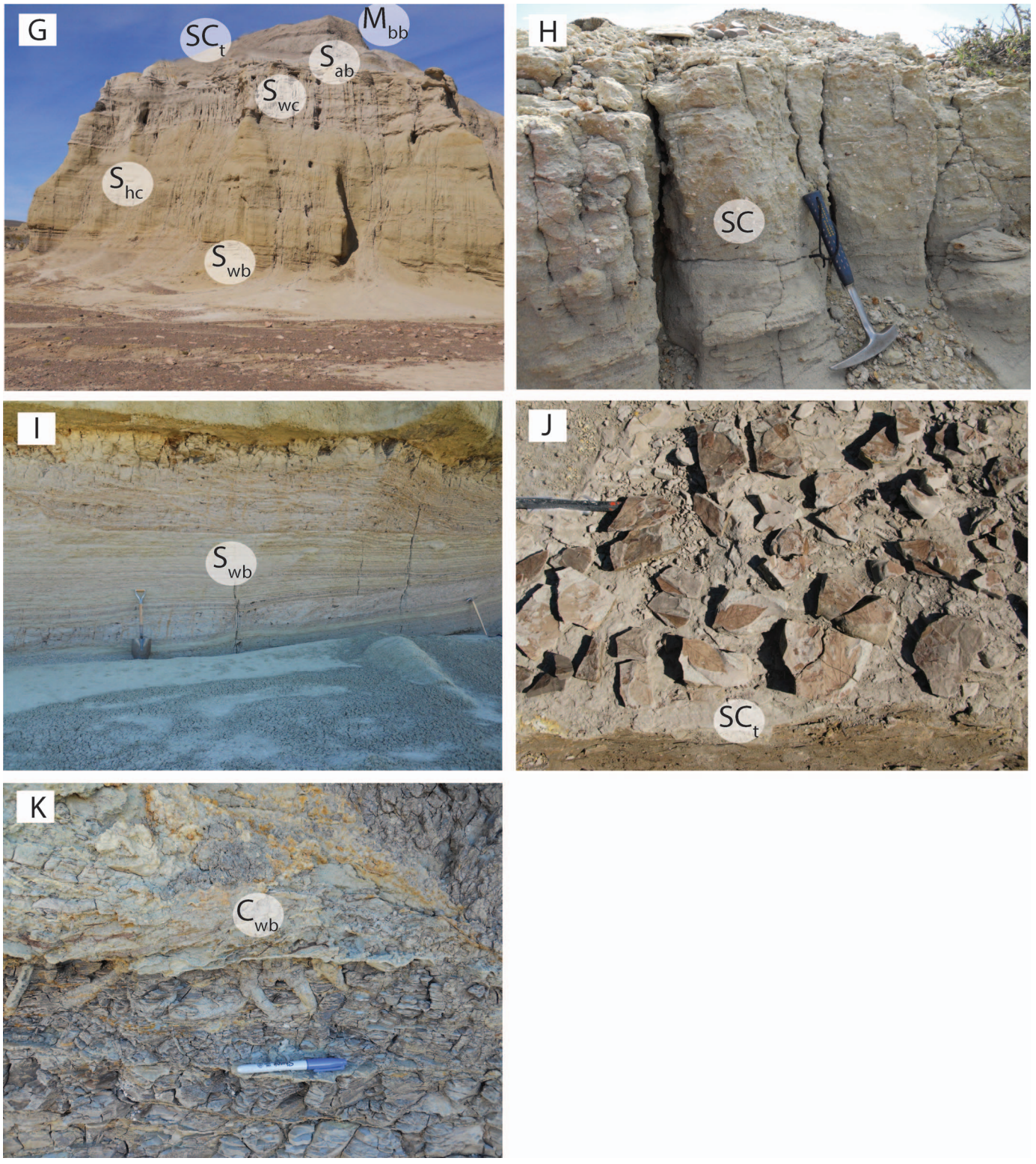

FIG. 5.—*Continued.*

where *h* represents point bar thickness (Crerar and Arnott 2007). Given a point bar thickness of 2–4 m and a dip of 10–15°, the width of these tidal channels was on the order of 50–150 m. Plant fossils within this facies occur mostly in the muddy beds; they are well preserved, abundant, and interpreted as parautochthonous (e.g., Gastaldo and Huc 1992).

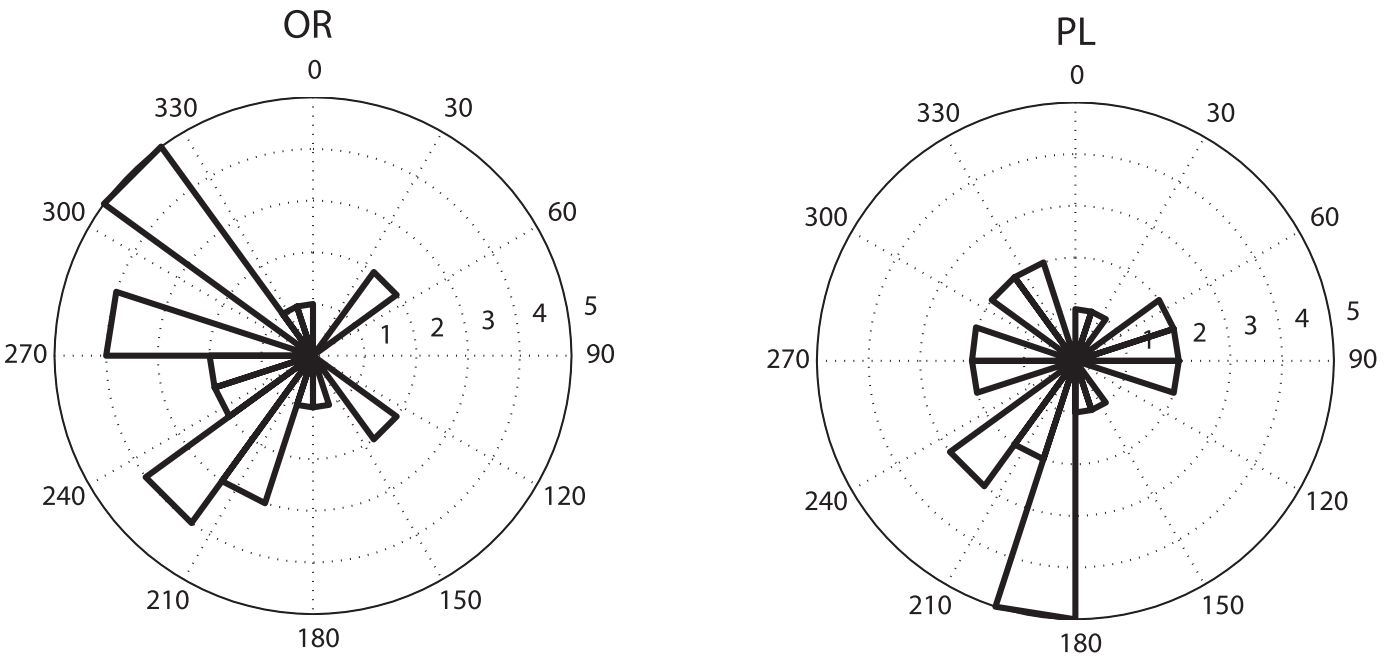

FIG. 6.—Rose diagrams showing paleocurrent directions of facies S_{wc} at Ormachea Park (OR, left) and Palacio de los Loros (PL, right). Zero degrees = True North. Paleocurrents cluster to the NW and SW.

Facies SC_t*: Transitional Sandstones to Silty Clay Shales*

Description.—Facies SC_t (Fig. 5J) is a poorly to moderately cemented lithic wacke interbedded with silty clay shales. The sand is poorly to moderately sorted, with a median grain size of vf-fU, and is composed of 60–80% sub-rounded to rounded quartz grains (observed by hand lens). Fine laminations near its base are replaced by mottling in higher sections. Silty clay shale beds become more abundant up-section. The lower and upper contacts are transitional. The silty clay contains plant rhizoliths, mottling, and pedogenic slickensides. This facies is present at both PL and OR and lies above either facies S_{wc} or facies S_{ab}. A sample from this facies at PL shows the presence of *Pediastrum boryanum* spores, a type of freshwater green algae (Clyde et al. 2014). Facies SC_t ranges in thickness from absent to 10 m and is the host for fossil plant locality PL-2, where the floras are particularly well preserved, as well as PL-5.

X-ray diffraction of clays from facies SC_t shows significant clay mineral peaks at 14, 10, and 7 Å that are identified as smectite, illite/glauconite, and a kaolin-mineral, respectively. The 14 Å peak possesses the highest intensity clay peak in all 20 samples, suggesting that the clay fraction of these samples is strongly dominated by smectite (Fig. 3). The 10 Å peak most likely represents a mixed-layer clay containing both glauconite and illite. This is not a pronounced peak and disappears stratigraphically upward into the larger 14 Å smectite peak (Fig. 3). The 7 Å peak identifies the presence of either kaolinite or halloysite. The TOC values in this facies range between 0.1–0.32 %, the highest values of any facies.

Interpretation.—Facies SC_t is interpreted as a paleosol developed in swales between the point-bar ridges of tidally-influenced fluvial channels on a prograding lower coastal plain, or in muddy plugs of abandoned tidal channels. Fine grain sizes and laminations indicate a very low energy environment, and mottling is interpreted to result from periodic wetting (Coventry and Williams 1984). Stratigraphic variations in the frequencies of rhizoliths, slickensides, and mottling indicate that sedimentation was episodic, as might occur from very infrequent flooding. The presence of *Pediastrum boryanum* (Clyde et al. 2014) provides evidence of freshwater input and proximity to land. This facies sits on and is occasionally replaced laterally by facies S_{ab}, suggesting that it arises from preferential, fine-grained deposition in swales or abandoned channels.

The clay mineralogy, roots, mottling, slickensides, and internal fabric of facies SC_t in its lower part describe a Gleysol, i.e., a soil produced under conditions of poor drainage according to the Mack et al. (1993) paleosol classification system. The dominance in this facies of montmorillonite, a clay mineral within the smectite group, indicates an environment that was poorly drained, such as wetlands (Singer 1980; Borchardt 1989). Smectites are also common minerals in weathered volcanic ashes and are the weathering product of mafic rocks (Borchardt 1989; Chamley 1989), such as the Cretaceous La Angostura Basalt. Facies SC_t becomes mottled and weathered upward; the top few meters are classified as a Vertisol, i.e., a paleosol with greater than 30% clay and deep cracks from repeated wetting and drying. The 10 Å peak weakens up-section (Fig. 3), indicating secondary alteration and transformation of smectite into illite, or the presence of transported glauconite in the samples. Wetting and drying cycles, represented by the mottling, help incorporate potassium and aluminum in sediments which may lead to their illitization (Fanning et al. 1989). The occurrence of kaolinite and halloysite in facies SC_t suggests a protolith of volcanic ash and rock fragments subjected to weathering (Singer 1980; Allen and Hajek 1989; Fanning et al.,1989; Joussein et al. 2005). Halloysite represents an intermediate stage in the transition of smectite to kaolinite (Chamley 1989; Dixon 1989), a transformation that occurs when soils undergo leaching. We conclude that SC_t in its lower part corresponds to a Gleysol (Mack et al. 1993); the top few meters is classified as a Vertisol based on an increase in mottling and weathering.

Facies C_{wb}*: Wispy Bedded Clay Shales*

Description.—Facies C_{wb} (Fig. 5K) consists of a finely laminated (1–3 mm) purplish gray clay shale interbedded with 1–3 cm long, 1–4 mm thick

sand wisps that decrease in number but increase in size up-section. The sand is vfU, light gray litharenite. This facies typically is 3–4 m thick. Burrows are absent except for the upper 5 to 10 cm, which contains 5 cm long, vertical U-shaped burrows (Fig. 5K) interpreted as the ichnogenus *Arenicolites*. Plant debris is abundant, and 3 cm long intact leaves occur in the upper strata. Weathering features include iron-oxide staining and gypsum formation. Facies C_{wb} contains benthic and planktonic foraminifera, palynomorphs, calcispheres, and a diverse assemblage of dinocysts (in sample OR1016 of Clyde et al. 2014). Facies C_{wb} appears in outcrop above facies *SC* (e.g., Fig. 4A; Dromedary Hill). It also occurs in the lower 4 m of the RG section.

Interpretation.—Undisturbed laminations indicate a low energy environment below storm wave-base. The presence of *Arenicolites* in the upper few cm of this facies indicates upward-shallowing. The dinocyst assemblage found in facies C_{wb} is typical of a Danian marine shelf (Clyde et al. 2014). Macrofloral presentation is poor and limited within this facies, suggesting lengthy transport fitting the deep water interpretation.

Facies M_{bb}*: Brownish Black Mudstones (Banco Negro Inferior)*

Description.—Facies M_{bb} is a mottled brownish black mudstone with pedogenic slickensides, iron nodules, rhizoliths, and other root traces (Figs. 3, 5F, 5G) that makes up the classic Banco Negro Inferior. Clay mineralogy mirrors facies SC_t, but montmorillonite is even more abundant. Values of TOC within this facies range between 0.1–0.26 %. Its basal contact is transitional, and its upper contact is the erosional unconformity with the base of the Peñas Coloradas Fm. of the Río Chico Group. Facies M_{bb} is generally tabular and 2 to 3 m thick. It is a widespread unit, found locally in PL and OR, and regionally across the San Jorge Basin. Along the coast, it is the source of the Peligran vertebrate assemblage (see Introduction).

Interpretation.—Facies M_{bb}, equivalent to the BNI, is interpreted to have been deposited in a widespread coastal-plain lowland forest that was seasonally waterlogged or flooded. The extensive paleosol development indicates a low sedimentation rate. Vertebrate faunas from the coastal BNI, including frogs, diverse turtles, crocodilians, and a monotreme (Pascual et al. 1992; Bonaparte et al. 1993; Sterli and de la Fuente 2012), support a terrestrial, waterlogged environment. The dark coloration of the BNI that gives it its name is correlated to high aluminum content (~ 23 %) in relation to halloysite, and not to carbon or manganese content.

Abundant mottling, gray coloration, dominance of smectite, and slickensides identify much of the BNI as a Vertisol similar to the upper portion of facies SC_t, supporting the idea of conformable facies transitions in the uppermost Salamanca Fm. Similar black paleosols occur in Paleocene sediments of Texas that also contain slickensides, low TOC values (0–2%), rare carbonate nodules, and a clay mineral fraction dominated by smectite with a lesser kaolinite presence (White and Schiebout 2008). These paleosols were also interpreted to have formed in a seasonally waterlogged environment. A similar setting possibly comprised the paleoenvironment of the Peligran vertebrate assemblage, if the features of the coastal BNI exposures, not studied here, are found to be similar.

FACIES ASSOCIATIONS

The twelve facies described above can be organized into a typical eustatic sequence stratigraphic framework (Figs. 7, 8). The transgressive lag deposits of facies SC everywhere in the study area sit on an erosional unconformity that separates Paleogene from Cretaceous sedimentary strata. We take this unconformity to be a sequence boundary (SB-1 in Fig. 8), and facies SC to be the transgressive systems tract (TST). Above the transgressive lag deposits of facies SC is always found facies C_{wb}, a faintly laminated, wispy burrowed clay shale that we interpret as a mid- to outer-shelf deposit. The position of the maximum marine flooding surface (mmfs), and, therefore, the boundary between the transgressive and highstand systems tracts, is difficult to define. However, based on dinoflagellate cysts and other microfossils from facies C_{wb} that indicate normal marine conditions (Clyde et al. 2014), we place it in facies C_{wb}. We interpret the transition from shelf mud shale of facies C_{wb} to reworked, deep water and subtidal bars of facies S_{shc}, S_{wb}, and S_{hc}, respectively, as a HST deposited during progradation of the shoreline while sediment influx to the basin overwhelmed accommodation space. The bases of the shallow tidal bars of facies S_{wc} (Figs. 4A, B) represent an erosional sequence boundary (SB-2) that is observed in the study area and reported to increase in relief on the Atlantic Coast (Legarreta and Uliana 1994). Shallow tidal bars, sand flats, laterally accreting point bars, and muddy tidal flats of facies S_{wc}, S_{ppl}, S_{ab}, and SC_t, respectively, sit above SB-2 and are interpreted as a lowstand systems tract (LST) of tidal channel fills and nearshore bars that give way upwards to finer-grained sandstones and mud shale of a thin transgressive systems tract. The latter are considered a TST rather than a continuation of the LST because accretion sets, laminated silt shale, and well preserved floras within facies SC_t indicate a period of aggradation under lower energy flows.

Facies M_{bb}, the Banco Negro Inferior, caps the Salamanca Fm. and is interpreted as a HST that slowly prograded towards the Atlantic Coast. The environment of deposition was a seasonally waterlogged, coastal lowland forest. The Salamanca Fm. is succeeded by another sequence boundary (SB-3 in Fig. 8), separating it from the superjacent, fluvial Peñas Coloradas Fm.

PROVENANCE

Where were the source terrains that provided the sediment delivered to our fossiliferous field area in the San Jorge Basin? To address this question, sandstones of the Salamanca Fm. were collected for compositional analysis from the sections at Dromedary Hill in OR (Fig. 4), PL, and from the PC Formation at LF. The sands of the younger, basal Peñas Coloradas Fm. at LF were included for comparison because of their macrofloral content. Grain size often exerts a strong effect on sand composition, but over the range of sizes sampled, we found no obvious relationship between grain size and lithic content.

The Salamanca sandstones range between feldspathic litharenites and litharenites (Fig. 9). Samples from OR and PL lie within the recycled orogen provenance in the Dickinson classification system (Dickinson et al. 1983) due to their intermediate quartz content, high sedimentary, low carbonate, and low volcanic lithic fragments, and their low feldspar content. Quartz grains from these localities show straight extinction, and metamorphic lithics are rare, implying that these sediments came from a plutonic rather than a strongly metamorphosed and tectonically complex area. The North Patagonian batholith is a likely source terrain. It lies about 250 km west of the field area and was uplifted and eroded during the Late Cretaceous (Uliana and Biddle 1988; Folguera et al. 2011).

The sandstones at Las Flores (LF) were sampled just above the plant locality within the Peñas Coloradas Fm. They contain abundant feldspar, few sedimentary lithics, and approximately 50% volcanic lithics. The majority of the lithics are lathwork volcanic fragments. The combination places them in the undissected to transitional magmatic arc category (Fig. 9). The San Bernardo fold belt, to the immediate west, is a possible source terrain because it was subject to uplift and magmatism as early as the Late Cretaceous, and it is the nearest known volcanic source to the LF section (Folguera et al. 2011). Also, within the San Bernardo range, the Peñas Coloradas Fm. directly overlies Cretaceous rocks (Raigemborn et al. 2014). Indeed, Quartz, Feldspar, Lithic (QFL) ternary diagrams of the Late Cretaceous Bajo Barreal sandstones from fluvial facies at two sites bordering the San Bernardo Range, 35–75 km west and northwest of OR

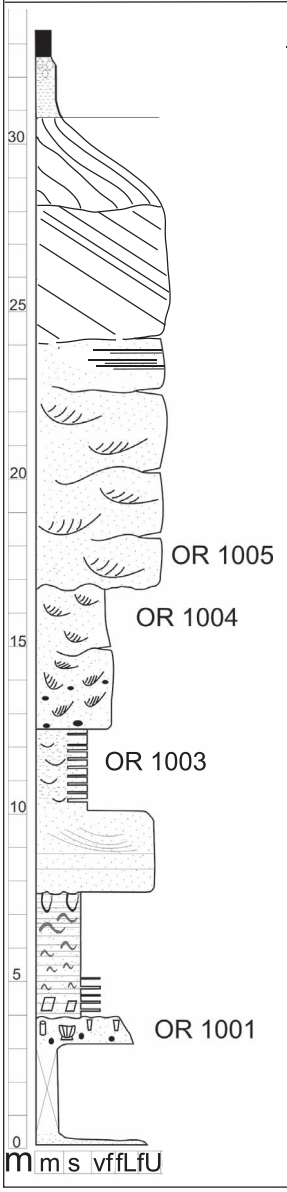

Graphic Log (scale in m)	Facies	Description	Paleoenvironmental Interpretation	Systems Tracts
	M_{bb}	Brownish black mud	Widespread coastal swamp	HST TST
	SC_t	Transitional sands to silty clay	Abandoned tidal channel fill	
	S_{ab}	Accretion-bedded sand & silt	Tidal channel point bars	
	S_{uc}	Unidirectional cross-bedded sands	Tidal runoff micro-deltas	
	S_{ppl}	Planar laminated sand	Sand flats	LST
	S_{wc}	White cross-bedded sand	Tidal bars deposited in tidal channels near head of estuary	
	S_{hc}	Heterolithic cross-bedded sand	Subtidal bars on a sand shoal containing mutually evasive ebb and flood channels	SB-2
	S_{wb}	Wavy-bedded sand and silt	Deeper water tidal bars	
	S_{shc}	Swaley-hummocky cross-bedded sand	Reworked tidal bars	HST
	C_{wb}	Wispy-bedded clay	Low-energy shelf muds	mmfs
	SC	Poorly sorted litharenites and clay	Foreshore transgressive lag	TST
				SB-1

FIG. 7.—Summary facies sequence and interpreted paleoenvironments and systems tracts, based on composite section at Ormachea Park (see Table 1 and Fig. 4 for legend). OR1001 to 1005 indicate locations of petrography samples at Dromedary Hill.

and PL (Umazano et al. 2009), closely resemble QFL values at the LF locality. Due to quartz roundness, it is possible that LF sandstones from the Peñas Coloradas Fm. are composed of reworked volcanic lithics of the Bajo Barreal Fm. However, distinct compositional differences between Bajo Barreal and Salamanca sands show that with the exception of facies *SC*, Salamanca sands at PL and OR do not represent reworking of the subjacent strata. Finally, previous petrographic work conducted in the Peñas Coloradas Fm., 100–150 km northeast of our sections (Raigemborn 2006), indicated a dissected to transitional magmatic arc provenance to the northwest of that study area with progressive unroofing of underlying batholithic rocks, similar to our findings from the LF section.

ORIGIN OF THE STRONG TIDES

The environmental interpretations of the Salamanca Fm. presented above require strong tidal flows in the San Jorge embayment. This is problematic because the weaker tides of the Paleocene Atlantic Ocean that was narrower than today, coupled with frictional damping in a relatively broad and shallow San Jorge paleo-estuary, might be expected to produce negligible tides in the study area. To test the conjecture of a meso-tidal origin for some facies, we modeled the paleo-San Jorge Basin using Delft3D, a hydrodynamic sediment transport model created by Deltares (Hibma et al. 2004; Lesser et al. 2004; Marciano et al. 2005; van Maren 2005).

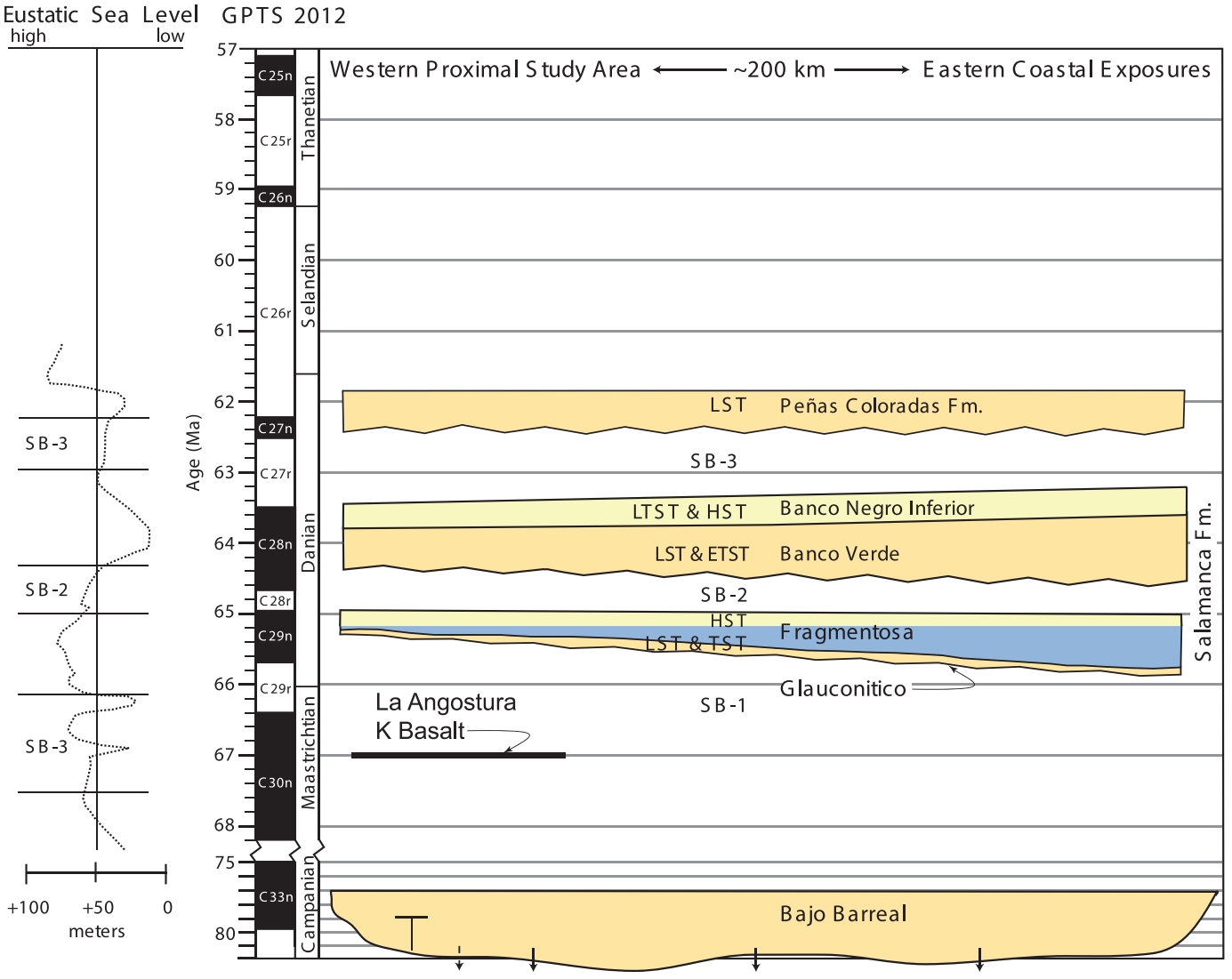

FIG. 8.—Wheeler diagram of stratigraphic events in the study area during the late Cretaceous through early Paleocene, modified from Clyde et al. (2014). Eustatic sea level curve from Kominz et al. (2008). Salamanca facies names after Feruglio (1949) and Bond et al. (1995). The basalt that lies between the Bajo Barreal and Salamanca formations is ^{40}Ar-^{39}Ar dated to 67.31 ± 0.55 Ma, and a tuff in the Peñas Coloradas Fm. at PL is U-Pb dated to 61.984 ± 0.041 (Clyde et al. 2014). SB = sequence boundary; LST = lowstand systems tract; TST = transgressive systems tract; HST = highstand systems tract; (E or L)TST = early or late transgressive systems tract, respectively.

In the absence of a detailed paleogeography and paleoclimatology for the San Jorge Basin, we used the present-day La Plata Estuary freshwater discharges and depths and the San Jorge Basin boundaries from Sylwan (2001) as guides. Thus, the modeled San Jorge Basin consists of a wide arcuate embayment open to the Atlantic and receiving freshwater influx from six eastward-flowing rivers, four with a mean annual discharge equal to 3,000 $m^3\ s^{-1}$ and two with a discharge equal to 4,000 $m^3\ s^{-1}$. The bathymetry varies linearly from 150 m at the Atlantic shelf edge to 3 m at its western end, consistent with other modern shallow continental embayments (Glorioso and Flather 1997). The Chezy friction factor is taken to be constant over the whole basin at 65 (Glorioso and Flather 1997), and the Coriolis parameter is computed for a paleolatitude of 45°S. At the open boundary with the Atlantic, an M2 shelf tide is prescribed with an amplitude of 80 cm, similar to modern M2 tides on the Patagonian shelf (Glorioso and Simpson 1994). Gravitational acceleration is taken at today's value, and water density is computed as a function of salinity, with the open ocean salinity set to today's average global value of 35 ppt.

Results of the tidal numerical model confirm that amplified tides were physically probable in the embayment (Fig. 10). Steady-state tidal ranges predicted by Delft3D in the headwaters of the arcuate San Jorge embayment are approximately three times the modern-day Atlantic tide, with declining amplification seaward.

How robust are these estimates in the face of uncertainties in the average bathymetry, east-west extent, and planform of the San Jorge Basin during the early Paleocene? The amplification in the simulations arises from three causes: horizontal convergence of the tidal wave crest, vertical convergence due to shallowing bathymetry, and resonance of the tidal wave in the San Jorge embayment. For frictionless wave propagation, the effects of horizontal and vertical convergence are given by Green's Formula as:

$$\frac{a_2}{a_1} = \left(\frac{l_1}{l_2}\right)^{1/2} \left(\frac{h_1}{h_2}\right)^{1/4} \quad (3)$$

where subscripts 1 and 2 denote two different locations in a converging

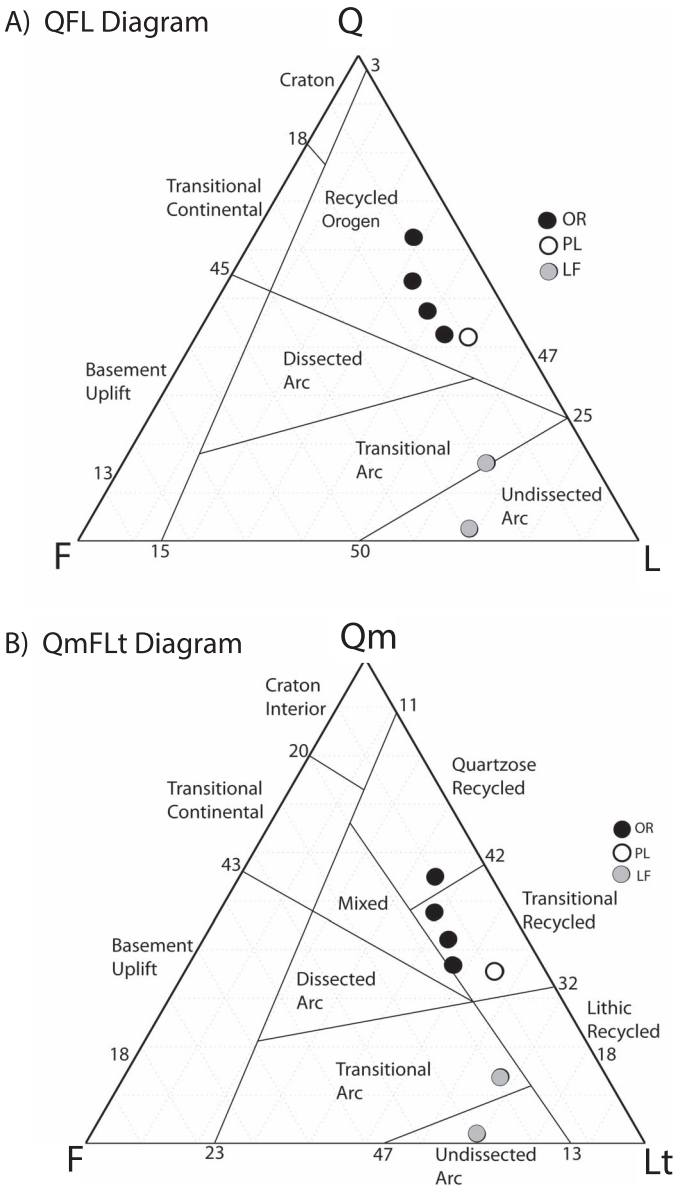

FIG. 9.—QFL and QmFLt diagrams of samples collected at PL, OR, and LF. **A**) QFL diagram based on the Dickinson et al. (1983) classification system; PL and OR samples lie within the recycled orogen domain, whereas LF samples lie within the undissected arc orogen domain. **B**) QmFLt diagram based on the Dickinson et al. (1983) classification system; PL and OR samples are classified as recycled orogen, whereas LF samples are classified as undissected arc and transitional arc orogens. Abbreviations: Q = total quartzose grains; F = monocrystalline feldspar grains; L = unstable polycrystalline lithic fragments of either igneous or sedimentary parentage, including metamorphic varieties; Qm = monocrystalline quartz; Lt = total polycrystalline lithic fragments including quartzose varieties.

embayment, a is the amplitude of a tidal wave, l is the width of the embayment into which the tidal wave is traveling, and h is the average still-water depth. Tidal wave amplitude rises as the square root of horizontal convergence and quarter root of shallowing water depth. A rectangular basin shoaling from an average of 100 m at the Atlantic shelf edge to 5 m produces an amplification in tidal range of about 2. Resonance arises when the distance from the edge of the continental shelf to the shoreline is a quarter wavelength of the semi-diurnal tidal wave (Godin 1993). Thus, the tides at the shoreline should be amplified by resonance when the width of the shelf and embayment W is equal to 1/4L, where the wavelength L of a tidal wave is given by:

$$L = \frac{2\pi\sqrt{(gh)}}{\sigma} \quad (4)$$

where h = the mean water depth of the shelf and embayment, and σ = the angular frequency of the tidal component in radians per second, which for an M2 tide equals 1.405×10^{-4} s^{-1}. For an average water depth of 25 m in the Paleocene San Jorge embayment, the resonant width equals approximately 175 km. As the estuary expanded and contracted with relative sea level during deposition of the Salamanca Fm., it seems probable that there would be intervals of tidal resonance, much as is occurring in the Bay of Fundy (Canada) today. Thus, we conclude that tides in the study area could reasonably have been in the high micro- to low meso-tidal range, consistent with the environmental interpretations based on outcrops.

SEQUENCE STRATIGRAPHIC INTERPRETATION

The Salamanca Fm., including the BNI, was deposited during three Danian paleomagnetic intervals—C29n, C28n, and in eastern outcrops C27r—during which the San Jorge Basin experienced positive accommodation (Fig. 8). Following an interval of erosion that started in the Late Cretaceous, a relative base level rise during Chron C29n created a widespread marine transgression (Figs. 8, 11). This base level rise is represented by the undulating marine flooding surface at the base of the Salamanca Fm. and facies of the subsequent lowstand and transgressive systems tracts. With continued positive accommodation, a broad, shallow estuary formed that extended at least as far as the San Bernardo belt, as evidenced by the offshore character of Salamanca facies in the study area at this time.

The maximum marine flooding surface that marks the beginning of the first HST is defined by clay shale deposits within facies C_{wb}, interpreted to be low energy, deeper water shelf deposits (Fig. 11). These clay shales are well laminated and unburrowed. Sandy and silty facies S_{hc}, S_{shc}, and S_{wb} represent later phases of the HST during late Chron C29n (Figs. 8, 11). An abundance of tidal indicators suggests that these facies were deposited within tens of km of the San Jorge paleo-estuary head. Rhythmic flaser and lenticular bedding of facies S_{wb} are characteristic of a tidal bar environment with little fluvial input (Zhang and Zhang 2008). Tidal- and storm-influenced facies S_{hc} and S_{shc} represent the upper portions of tidal sand bars that are dominated by bidirectional cross-bedding (Zhang and Zhang 2008). Fine to medium grain size and trough cross-bedding orientations indicate that these facies were dominantly formed by the ebb tides that generally flow through the central mid-channel of an estuary (Harris 1988; Dalrymple et al. 1990). The progressive fining-upward grain size of these facies, along with thin accretion beds and plant accumulations, suggest a progressive shoaling, as would occur with progradation of intertidal mudflats or abandoned channel fills proximal to a lowland coastal forest.

Following this highstand, a second sequence boundary (SB-2) formed during Chron C28r and probably during upper C29n and lower C28n (Fig. 8). We ascribe this erosion to a fall in the eustatic sea level curve, as per Kominz et al. (2008), possibly aided by the Paleocene extension of WNW-ESE trending normal faults observed by Foix et al. (2102b) in outcrop and seismic data. Earlier workers took the unconformity we interpret as SB-2 to be a local fluvial or tidal channel base. However, as argued in Clyde et al. (2014), the simplest interpretation of paleomagnetic, microfossil, and other chronologically informative data in the study area is that Chron C28r is entirely missing between the landward equivalents of the Fragmentosa and Banco Verde lithologic units of Feruglio (1949), which are roughly equivalent to our facies S_{hc} and S_{wc}, respectively. A significant regional unconformity at this horizon also

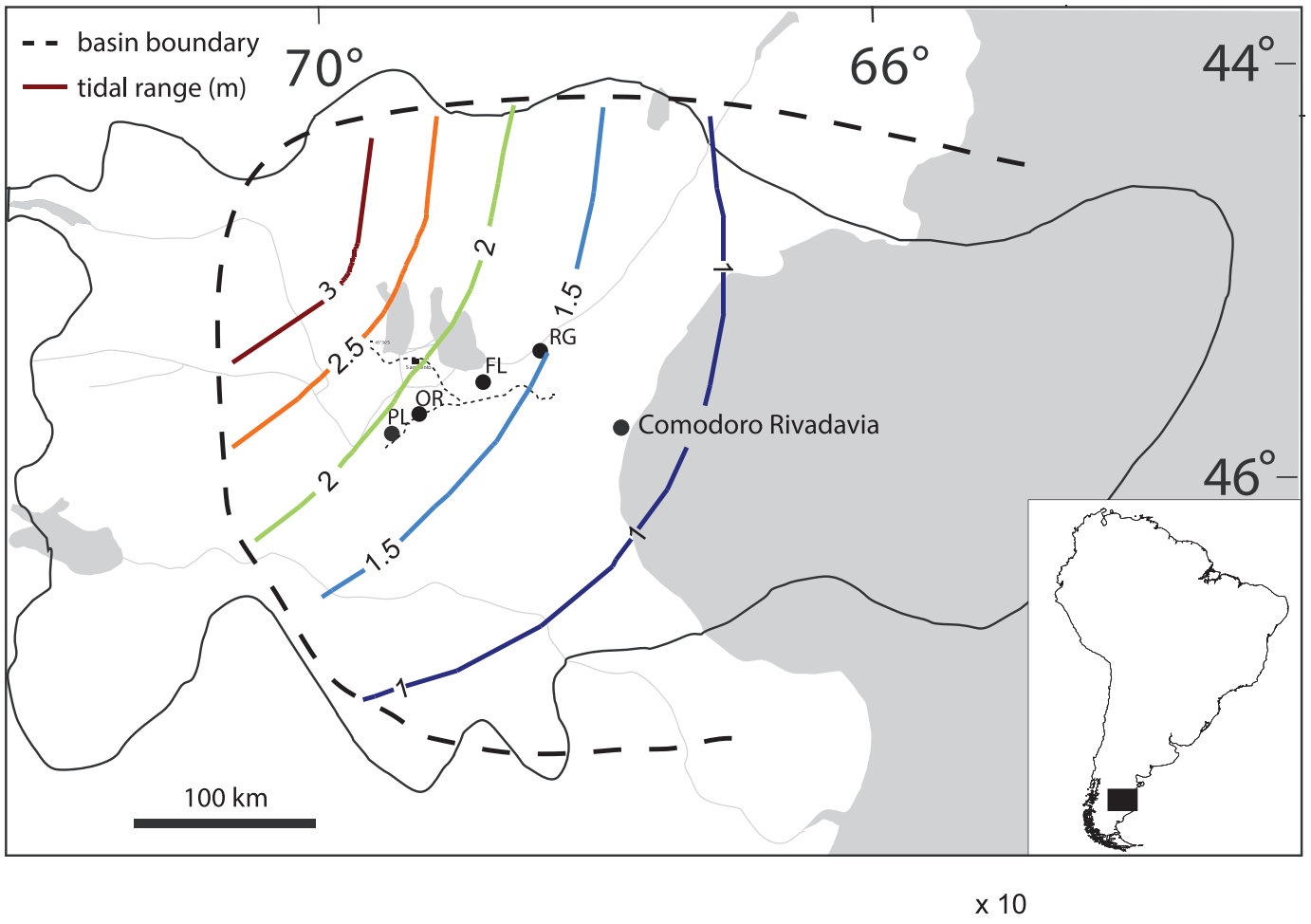

FIG. 10.—Modeled tidal range for the San Jorge Basin with an arcuate boundary and water depths decreasing landward from 150 m to 3 m. See text for details. A 1 m tide in the open proto-Atlantic amplifies to 3+ m in the embayment. Locality abbreviations given in Figure 1.

explains observations in the offshore Atlantic coast by Legarreta and Uliana (1994) and Foix et al. (2012b) that the base of the Banco Verde dramatically incises the subjacent Fragmentosa there.

Above SB-2 sit the fluvially influenced tidal channel deposits of facies S_{wc} and S_{uc} (Banco Verde equivalent). These deposits are interpreted as a lowstand systems tract formed when eustatic sea level stabilized during Chron C28n, and basin subsidence created positive accommodation space. The estuary began to fill through vertical accretion of channel sands and sand shoals (facies S_{wc}) and progradation of tidal flat muds (facies SC_t) and bayhead deltas (facies S_{uc}; Fig. 11). Facies S_{wc} is interpreted to have formed within the estuary head, where the tides caused river waters to store and release. Facies S_{uc} represents runoff microdeltas created by late ebb currents during low tide that infilled scours in facies S_{wc} (Dalrymple et al. 1990), or alternatively a bayhead delta. Mud drapes preserved on the lee sides of cross-beds indicate low-tide, slack-water deposits within the subtidal zone (Fenies et al. 1999). These deposits contain sets of "tidal bundles", where the sandy deposits wedged in between these mud drapes represent an ebb-flood cycle (Tape et al. 2003). The plane-parallel laminations of S_{ppl} represent upper-flow regime deposits of bar tops. These sediments represent the highest energy paleo-flows and the most proximal channel deposits of the Salamanca Fm. (Dalrymple et al. 1990,1992). The exceptional macroflora at PL-2 was deposited in tidal flat swales formed between the point-bar ridges of tidally-influenced fluvial channels meandering across the flats (facies SC_t).

Unlike earlier authors who interpreted the BNI (our facies M_{bb}) as a falling stage systems tract, we interpret it as a late transgressive and highstand systems tract (Fig. 8). Based on its facies characteristics, new chronologic constraints, and the Kominz et al. (2008) sea level curve, we argue that relative sea level rise during the time of facies M_{bb} was modest, producing not a significant marine transgression but a rising groundwater table and a decline in river slopes. These factors promoted a reduction in sediment delivery to the basin and the development of a widespread coastal forest that accumulated mottled pedogenic brown-black muds with a clay mineral assemblage indicative of a seasonally water-logged environment, consistent with the ecology of the Peligran vertebrate assemblage.

Because Chron C27r is missing between the BNI and the Peñas Coloradas Fm., we interpret the erosional unconformity between these units as another sequence boundary (SB-3). Foix et al. (2013) studied the Peñas Coloradas and higher formations near the coast and found two styles of deposition—braided channels with a high rate of aggradation, and low-sinuosity, meandering channels with a low rate of aggradation. These two fluvial architectures are attributed to variation in rates of subsidence and sediment supply, under the assumption of constant climate across the San Jorge Basin (Foix et al. 2013).

ENVIRONMENTAL INTERPRETATIONS OF PLANT LOCALITIES

The paleobotanical localities of interest and their associated sedimentary facies and ages are indicated in Figure 4 and Table 2. Macrofossils

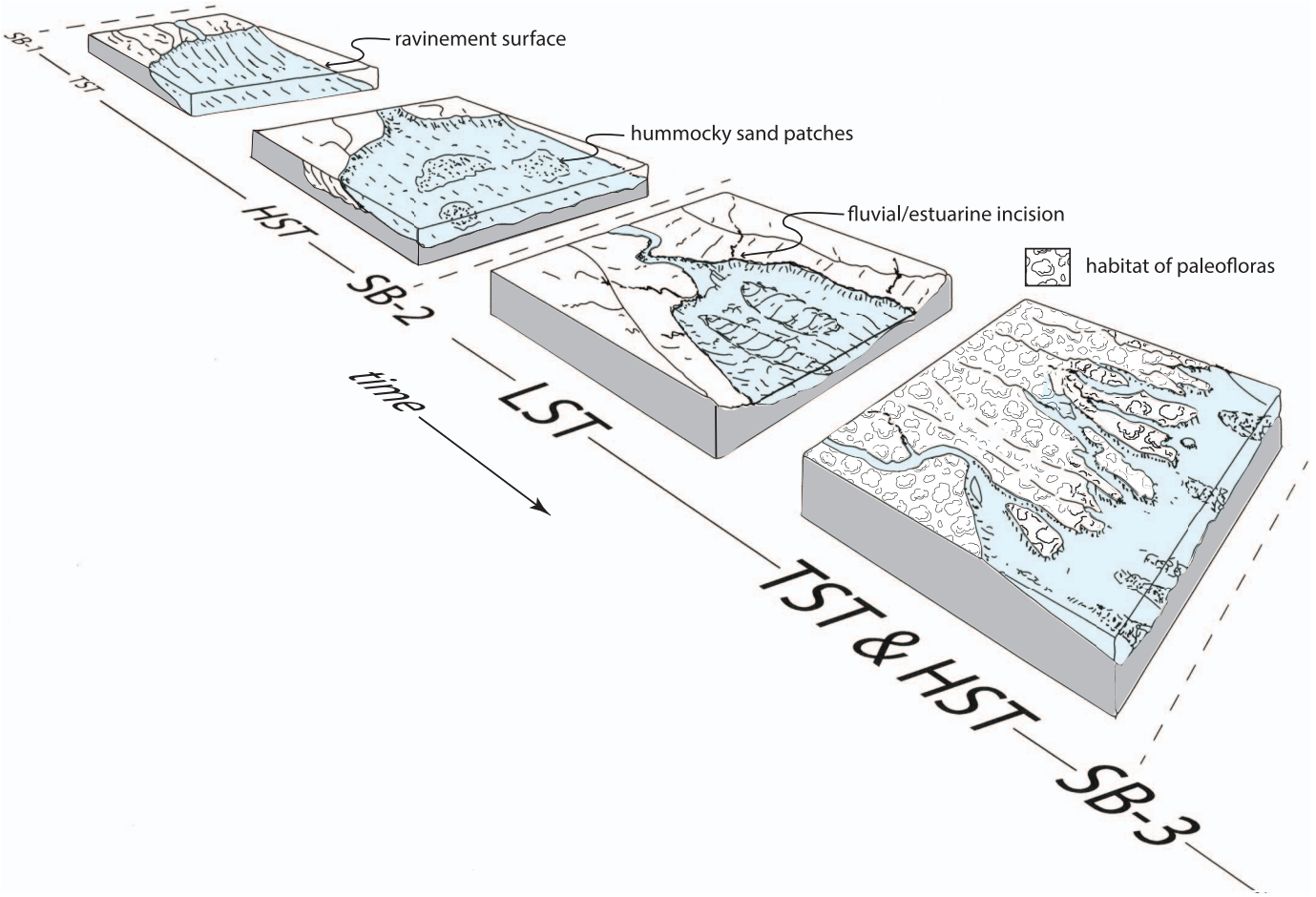

FIG. 11.—Schematic depositional model for the Salamanca Fm. in the study area. Abbreviations: SB = sequence boundary; TST = transgressive systems tract; HST = highstand systems tract; LST = lowstand systems tract. Detailed chronology of systems tracts given in Figure 9. Plant remains occur in many of the settings shown here; the superior preservation found at locality PL-2 corresponds to the legend item "habitat of paleofloras".

occur in estuarine deposits of the Salamanca Fm. in two principal settings that are stratigraphically separated—near the tops of subtidal bars composed of facies S_{hc} and S_{ab}, and within or above high-energy tidal bars of facies S_{wc} and S_{ab}. Plant macrofossils near the tops of facies S_{hc} and S_{ab} (sites OR-2, Cerro Solitario, PL-1, PL-3, PL-4, and RG) represent allochthonous deposits occurring below SB-2 at the end of a shallowing-upward cycle that caps the HST. These plant localities occur at an earlier time and in a different depositional environment from localities above the position of facies S_{wc} that lie above SB-2 (PL-2, PL-5, and OR-1). Note that this position of SB-2 is updated from what is shown in Clyde et al. (2014, Fig. 8), which placed all the plant compression localities above this unconformity. Given the new interpretation presented here, plant localities OR-2, Cerro Solitario, PL-1, PL-3, PL-4, and RG fall within Chron C29N instead of C28n, and they are at least ~ 300 ky older than previously proposed (Table 2).

The OR-2 and Cerro Solitario plant localities occur within a 10 cm-thick silt lens within subtidal bar deposits of facies S_{hc} that thins southward and is laminated in some areas, implying low flow energy, possibly during slack water. Plant deposits of OR-2 and Cerro Solitario represent the farthest transported fossil material. Fossil sites PL-1, PL-3, and PL-4 show evidence of the abandonment and infilling of high-energy tidal channels through accreting point bars represented by facies S_{ab}. Plant fossils at PL-1, PL-3, and PL-4 were preserved within siltstone beds of these point bars and tidal mud flats through some combination of transport by wind and tidal currents. The sequence boundary overlying these coastal plant deposits represents an erosive unconformity, followed by the LST.

Within high-energy tidal bar deposits of facies S_{wc} lie large, permineralized logs and stumps that are well known to visitors of Bosque Petrificado José Ormachea. These were transported through tidal channels and required the highest energy setting for transport. Plant deposits above facies S_{wc} and SB-2 (OR-1, PL-2, PL-5) are the most proximal to the plant source (Fig. 11). These are the youngest plant localities within the Salamanca Fm. (Chron C28n). Locality OR-1 occurs within S_{ab}; PL-2 and PL-5 occur within the sandstones, siltstones, and clay shales of facies SC_t that transition to the BNI (facies M_{bb}). Locality PL-2 specifically contains the best-preserved macroflora, shows the smallest amount of transport from the source, and can be interpreted as a parautochthonous assemblage. Fossil locality OR-1 occurs within a 6 m accretion-set consisting of intercalated thick sandstone and thin siltstone, with preserved macrofloras occurring in the siltstone beds. This set is interpreted as point bar accretion beds formed during the lateral migration of a tidally influenced, freshwater channel. Locality PL-5 occurs above the top of facies S_{uc} within a mud drape of facies SC_t. Mud drapes are common at PL-5, range in thickness from 10 – 50 cm, and occur on the foresets of coarse, trough-cross-bedded sandstone beds. Clay deposition is interpreted to occur during low-tide slackwater, with each sand-clay couplet representing one tidal cycle (Tape et al. 2003). The

TABLE 2.—*Fossiliferous facies and correlations to the geomagnetic polarity time scale (Gradstein et al. 2012) for each fossil-plant quarry.*

Plant quarry	Facies containing fossils	GPTS 2012
OR-1	S_{ab}	C28n
OR-2	S_{hc}	C29n
Cerro Solitario	S_{hc}	C29n
PL-1	S_{ab}	C29n
PL-2	SC_t	C28n
PL-3	S_{ab}	C29n
PL-4	S_{ab}	C29n
PL-5	SC_t	C28n
RG	S_{wb}	C29n
LF	*LF1*	C27n

floras at OR-1 and PL-5 are allochthonous; however, transport distance was less than a few kilometers.

The PL-2 quarry contains the most diverse, abundant, and well preserved macrofloras of those studied and includes many very fragile elements that could only survive negligible transport, such as attached compound leaves, whole leaves with in situ cuticles, flowers, infructescences and cones, and winged seeds, along with clam shells, insect wings, and bird feathers. This locality lies at the base of facies SC_t near the top of facies S_{wc}, a stratigraphic position representing the final stages of estuarine progradation and infilling. It is likely that PL-2 represents a muddy deposit along a low-energy, tidally influenced fluvial channel. These deposits are the most proximal of all to the plant source and represent parautochthonous accumulations from the vegetation proximal to the estuarine tidal flats (Fig. 11).

CONCLUSIONS

The Salamanca Fm. in our field area is underlain by a sequence boundary of approximately 10 million years duration. Following a Paleocene eustatic sea level rise, the San Jorge Basin was flooded from the east during Chron C29n, and accumulated lowstand, transgressive, and highstand systems tract deposits that compose the lower and middle Salamanca Fm. A lowering of Paleocene eustatic sea level created a second sequence boundary during Chron C28r, with progressively deeper incision to the east that was possibly caused by syndepositional reactivation of Cretaceous normal faults (Foix et al. 2012b). This sequence boundary was followed by a rise in eustatic sea level during Chron C28n that allowed the slow accumulation of tidal estuarine facies comprising the uppermost Salamanca Fm. The strong tidal flows along the western shore of the Paleocene San Jorge Basin estuary are predicted by a hydrodynamic model of amplified tides near the estuary head that arise from both shoreline convergence and tidal resonance. The last stage of Salamanca deposition is represented by paleosol deposits of the BNI, which are classified as gleyed vertisols and dominated by montmorillonite with illite, glauconite, and kaolin-minerals occurring in lesser proportion. We interpret the montmorillonite dominance to indicate a waterlogged environment created by a rising groundwater table within a lowland forest. A third drop in eustatic sea level during Chron C27r produced a third sequence boundary that marks the end of Salamanca deposition.

The landscapes that supported the diverse compression macrofloras of the Salamanca Fm. in the proximal portion of the San Jorge Basin grew in coastal lowland forests fringing a tidal estuary. Plant remains were preserved in abandoned tidal channel fills and prograding tidal flats along this micro- to meso-tidal estuary. An estuarine setting is supported by the mixture of aquatic, freshwater green algae and marine dinocysts found in many samples. The plant localities occur both below and above SB-2, and in five sedimentary environments: silty beds within accretion cross-bed sets of tidal bars, silt lenses within tidal channel sands, mud drapes on sandy tidal bars, muddy tidal flats, and within muddy deposits of low-energy tidal channels. The best-preserved paleofloral sites (PL-1 and especially PL-2) are interpreted as the most proximal to the source forest.

Our paleoenvironmental, geochronologic, and sequence stratigraphic interpretations provide a robust framework for comparative investigations of the composition, diversity, and taphonomy of the early Danian Salamanca Formation floras of Patagonia in the global contexts of Gondwanan evolutionary biogeography and recovery from the end-Cretaceous extinction.

ACKNOWLEDGMENTS

This research was funded by NSF grant DEB-0919071. We thank Secretaría de Cultura and Secretaría de Turismo y Áreas Protegidas of Chubut Province and Sarmiento City for access and research permits, the Visser, Salazar-Bochatey, Edna de Galáz, Porto, Martínez, and Balercia families for land access, and R. Cúneo, M. Caffa, L. Canessa, K. Johnson, P. Puerta, and E. Ruigómez for exceptional logistical assistance. This research partially completed requirements for a Masters in Geosciences for EEC at Pennsylvania State University, 2011.

REFERENCES

ALLEN, B.L., AND HAJEK, B.F., 1989, Mineral occurrence in soil environments, *in* Dixon, J.B. and Weed, S.B., eds., Minerals in Soil Environments (2nd ed.), Soil Science Society of America, Madison, WI, p. 199–278.

ANDREIS, R.R., MAZZONI, M.M., AND SPALLETTI, L.A., 1975, Estudio estratigráfico y paleoambiental de las sedimentitas Terciarias entre Pico Salamanca y Bahia Bustamante, provincia de Chubut, Republica Argentina: Revista de la Asociación Geológica Argentina, v. 30, p. 85–103.

ARCHANGELSKY, S., 1973, Palinología del Paleoceno de Chubut. I. Descripciones sistemáticas: Ameghiniana, v. 10, p. 339–399.

ARCHANGELSKY, S., 1976, Palinología del Paleoceno de Chubut. II. Diagramas polínicos: Ameghiniana, v. 13, p. 43–55.

ARCHANGELSKY, S. and ZAMALOA, M.C., 1986, Nuevas descripciones palinológicas de las Formaciones Salamanca y Bororó, Paleoceno de Chubut (República Argentina): Ameghiniana, v. 23, p. 35–46.

BARREDA, V.D., CÚNEO, N.R., WILF, P., CURRANO, E. D., SCASSO, R. A., AND BRINKHUIS, H., 2012, Cretaceous/Paleogene floral turnover in Patagonia: drop in diversity, low extinction, and a *Classopollis* spike: PLoS One, v. 7, e52455.

BELLOSI, E., PALAMARCZUK, S., BARREDA, V., SANAGUA, J., JALFIN, G., AND HERBST, R., 2000, Litofacies y palinología del contacto Grupo Chubut-Formación Salamanca en el oeste de la Cuenca Golfo San Jorge, Argentina: 11° Simposio Argentino de Paleobotánica y Palinología, Tucumán, Sep. 12–14, 2000, Resumenes, 9.

BERRY, E.W., 1937, A Paleocene flora from Patagonia: Johns Hopkins University Studies in Geology, v. 12, p. 33–50.

BERTELS, A., 1975, Bioestratigrafía del Paleoceno marino en la provincia del Chubut, Republica Argentina: Actas del I Congreso Argentino de Paleontología y Bioestratigrafía, Tucumán, v. 2, p. 271–316.

BLOTT, S.J., AND PYE, K., 2001, GRADISTAT: a grain size distribution and statistics package for the analysis of unconsolidated sediments, Earth Surface Processes and Landforms, v. 26, p. 1237–1248.

BONA, P., 2007, Una nueva especie de *Eocaiman* Simpson (Crocodylia, Alligatoridae) del Paleoceno Inferior de Patagonia: Ameghiniana, v. 44, p. 435–445.

BONAPARTE, J.F., AND MORALES, J., 1997, Un primitivo Notonychopidae (Litopterna) del Paleoceno inferior de Punta Peligro, Chubut, Argentina: Estudios Geológicos, v. 53, p. 263–274.

BONAPARTE, J.F., VAN VALEN, L.M., AND KRAMARTZ, A., 1993, La fauna local de Punta Peligro, Paleoceno inferior, de la provincia del Chubut, Patagonia, Argentina: Evolutionary Monographs, v. 14, p. 1–61.

BOND, M., CARLINI, A., GOIN, F., LEGARRETA, L., ORTIZ-JAUREGUIZAR, E., PASCUAL, R., AND ULIANA, M., 1995, Episodes in South American land mammal evolution and sedimentation: testing their apparent concurrence in a Paleocene succession from central Patagonia: Actas del VI Congreso Argentino de Paleontología y Bioestratigrafía, Trelew, p. 47–58.

BORCHARDT, G., 1989, Smectites, *in* Dixon, J.B. and Weed, S.B, eds., Minerals in Soil Environments (2nd ed.), Soil Science Society of America, Madison, WI, p. 675–727.

BOYD, R., DALRYMPLE, R., AND ZAITLIN, B., 1992, Classification of clastic coastal depositional environments, Sedimentary Geology, v. 80, p. 139–150.

BREA, M., MATHEOS, S., ZAMUNER, A., AND GANUZA, D., 2005, Análisis de los anillos de crecimiento del bosque fósil de Victor Szlápelis, Terciario Inferior del Chubut, Argentina: Ameghiniana, v. 42, p. 407–418.

BREA, M., MATHEOS, S., RAIGEMBORN, M. S., IGLESIAS, A., ZUCOL, A. F., AND PRÁMPARO, M., 2007, Aspectos paleoecológicos y paleoambientales del Bosque Petrificado Ameghino (Daniano), Chubut, Argentina: 4th European Meeting on the Palaeontology and Stratigraphy of Latin America. Cuadernos del Museo Geominero, v. 8, p. 45–50.

Brea, M., Zamuner, A., Matheos, S., Iglesias, A., and Zucol, A., 2008, Fossil wood of the Mimosoideae from the early Paleocene of Patagonia, Argentina: Alcheringa, v. 32, p. 427–441.

Brea, M., Matheos, S., Raigemborn, M., Iglesias, A., Zucol, A., and Prampáro, M., 2011, Paleoecology and paleoenvironments of podocarp trees in the Ameghino Petrified forest (Golfo San Jorge Basin, Patagonia, Argentina): constraints for early Paleogene paleoclimate: Geologica Acta, v. 9, p. 1–23.

Chamley, H., 1989, Clay Sedimentology, Springer-Verlag, New York, 623 p.

Choi, K. S., Dalrymple, R. W., Chun, S. S., and Kim, S.-P., 2004, Sedimentology of modern, inclined heterolithic stratification (IHS) in the macrotidal Han River Delta, Korea: Journal of Sedimentary Research, v. 74, p. 677–689.

Clyde, W. C., Wilf, P., Iglesias, A., Slingerland, R. L., Barnum, T., Bijl, P. K., Bralower, T. J., Brinkhuis, H., Comer, E. E., Huber, B. T., Ibañez-Mejia, M., Jicha, B. R., Krause, M., Schueth, J. D., Singer, B. S., Raigemborn, M. S., Schmitz, M. D., Sluijs, A., and Zamaloa, M. C., 2014, New age constraints for the Salamanca Formation and lower Río Chico Group in the western San Jorge Basin, Patagonia, Argentina: implications for K/Pg extinction recovery and land mammal age correlations: Geological Society of America Bulletin, v. 126, p. 289–306.

Coventry, R.J., and Williams, J. 1984, Quantitative relationships between morphology and current soil hydrology in some Alfisols in semiarid tropical Australia: Geoderma, v. 33, p. 191–218.

Crerar, E. E., and Arnott, R.W.C., 2007, Facies distribution and stratigraphic architecture of the Lower Cretaceous McMurray Formation, Lewis Property, northeastern Alberta: Bulletin of Canadian Petroleum Geology, v. 55, p. 99–124.

Dalrymple, R. W., Knight, R. J., Zaitlin, B. A., and Middleton, G. V., 1990, Dynamics and facies model of a macrotidal sand-bar complex, Cobequid Bay—Salmon River Estuary (Bay of Fundy): Sedimentology, v. 37, p. 577–612.

Dalrymple, R. W., Zaitlin, B. A., and Boyd, R., 1992, Estuarine facies models—conceptual basis and stratigraphic implications: Journal of Sedimentary Petrology, v. 62, p. 1130–1146.

Dickinson, W. R., and Suczek, C. A., 1979, Plate tectonics and sandstone compositions: AAPG Bulletin, v. 63, 2164–2182.

Dickinson, W. R., Beard, L. S., Brakenridge, G. R., Erjavec, J. L., Ferguson, R. C., Inman, K. F., Knepp, R. A., Lindberg, F. A., and Ryberg, P. T., 1983, Provenance of North American Phanerozoic sandstones in relation to tectonic setting: Geological Society of America Bulletin, v. 94, p. 222–235.

Dixon, J., 1989, Kaolin and serpentine group minerals, *in* Dixon, J.B. and Weed, SB., eds., Minerals in Soil Environments (2nd ed.), Soil Science Society of America, Madison, WI, p. 467–525.

Escapa,I.H., Iglesias, A., Wilf, P., and Cúneo, N.R., 2013, Oldest macrofossil record of *Agathis* (Araucariaceae), early Paleocene of Patagonia, Argentina, and its evolutionary significance: Botany 2013, New Orleans, abstract 378.

Fanning, D.S., Keramidas, V.Z., and El-Desoky, M.A., 1989, Micas, *in* Dixon, J.B. and Weed, SB., eds., Minerals in Soil Environments (2nd ed.), Soil Science Society of America, Madison, WI., p. 551–634.

Fenies, H., De Resseguier, A., and Tastet, J.-P., 1999, Intertidal clay-drape couplets (Gironde estuary, France): Sedimentology, v. 46, p. 1–15.

Farrell, K.M., Harris, W.B., Mallinson, D.J., Culver, S.J., Riggs, S.R., Pierson, J., Self-Trail, J.M., and Lautier, J.C., 2012, Standardizing texture and facies codes for a process-based classification of clastic sediment and rock: Journal of Sedimentary Research, v. 82, p. 364–378.

Feruglio, E., 1949, Descripción Geológica de la Patagonia, vol. I.: Ministerio de Industria y Comercio de la Nacion, Dirección General de Yacimientos Petroliferos Fiscales, Buenos Aires, Argentina, 334 p.

Foix, N., Foster, M., Allard, J.O., Paredes, J.M., Giacosa, R.E., Iovine, G., and Espinach, S., 2012a, Depósitos deltaicos de la Formación Salamanca (Paleoceno): un nuevo modelo sedimentario a partir de información de subsuelo y afloramiento, cuenca del Golfo San Jorge: XIII Reunión Argentina de Sedimentología, Salta, Argentina, Actas, p. 83–84.

Foix, N., Paredes, J.M., and Giacosa, R.E., 2012b, Upper Cretaceous–Paleocene extensional phase in the Golfo San Jorge basin (Argentina): growth-fault model, paleoseismicity and paleostress analysis: Journal of South American Earth Sciences, v. 33, p. 110–118.

Foix, N., Paredes, J.M., and Giacosa, R.E., 2013, Fluvial architecture variations linked to changes in accommodation space: Río Chico Formation (late Paleocene), Golfo San Jorge basin, Argentina: Sedimentary Geology, v. 294, p. 342–355.

Folguera, A., Orts, D., Spagnuolo, M., Vera, E.R., Litvak, V., Sagripanti, L., Ramos, M.E., and Ramos, V. A., 2011, A review of Late Cretaceous to Quaternary palaeogeography of the southern Andes: Biological Journal of the Linnean Society, v. 103, p. 250–268.

Folk, R.L., Andrews, P.B., and Lewis, D.W., 1970, Detrital sedimentary rock classification and nomenclature for use in New Zealand: New Zealand Journal of Geology and Geophysics, v. 13, p. 937–968.

Gastaldo, R. A., and Huc, A. Y., 1992, Sediment facies, depositional environments, and distribution of phytoclasts in the Recent Mahakam River delta, Kalimantan, Indonesia: PALAIOS, p. 574–590.

Gelfo, J.N., and Pascual, R., 2001, *Peligrotherium tropicalis* (Mammalia, Dryolestida) from the early Paleocene of Patagonia, a survival from a Mesozoic Gondwanan radiation: Geodiversitas, v. 23, p. 369–379.

Gelfo, J.N., Ortiz-Jaureguizar, E., and Rougier, G.W., 2007, New remains and species of the "condylarth"genus *Escribania* (Mammalia: Didolodontidae) from the Palaeocene of Patagonia, Argentina: Earth and Environmental Science Transactions of the Royal Society of Edinburgh, v. 98, p. 127–138.

Glorioso, P. D., and Flather, R. A., 1997, The Patagonian shelf tides: Progress in Oceanography, v. 40, p. 263–283.

Glorioso, P. D., and Simpson, J. H., 1994, Numerical modelling of the M_2 tide on the northern Patagonian shelf: Continental Shelf Research, v. 14, p. 267–278.

Godin, G., 1993, On tidal resonance: Continental Shelf Research, v. 13, p. 89–107.

Gradstein, Felix M, Ogg, Gabi, and Schmitz, M., eds.,2012, The Geologic Time Scale 2012: Elsevier, Amsterdam, 1144 p.

Harris, P.T., 1988, Large-scale bedforms as indicators of mutually evasive sand transport and the sequential infilling of wide-mouthed estuaries: Sedimentary Geology, v. 57, p. 273–298.

Hibma, A., Schuttelaars, H. M., and de Vriend, H.J., 2004, Initial formation and long-term evolution of channel-shoal patterns: Continental Shelf Research, v. 24, p. 1637–1650.

Iglesias, A., 2007, Estudio Paleobotánico, Paleocológico y Paleoambiental en Secuencias de la Formación Salamanca, del Paleoceno Inferior en el Sur de la Provincia de Chubut, Patagonia, Argentina, Ph.D. thesis, Universidad Nacional de La Plata.

Iglesias, A., Wilf, P., Johnson, K.R., Zamuner, A.B., Cúneo, N.R., Matheos, S.D., and Singer, B.S., 2007, A Paleocene lowland macroflora from Patagonia reveals significantly greater richness than North American analogs: Geology, v. 35, p. 947–950.

Jones, T., A, 2006, MATLAB functions to analyze directional (azimuthal) data—I: Single-sample inference: Computers and Geosciences, v. 32, p. 166–175.

Joussein, E., Petit, S., Churchman, J., Theng, B., Righi, D., and Delvaux, B., 2005, Halloysite clay minerals—a review: Clay Minerals, v. 40, p. 383–426.

Kominz, M., Browning, J., Miller, K., Sugarman, P., Mizintseva, S., and Scotese, C., 2008, Late Cretaceous to Miocene sea-level estimates from the New Jersey and Delaware coastal plain coreholes: an error analysis: Basin Research, v. 20, p. 211–226.

Krause, J.M., and Piña, C.I., 2012, Reptilian coprolites in the Eocene of central Patagonia, Argentina: Journal of Paleontology, v. 86, p. 527–538.

Leclair, S.F., 2002, Preservation of cross-strata due to the migration of subaqueous dunes: an experimental investigation: Sedimentology, v. 49, p. 1157–1180.

Leeder, M.R., 2011, Sedimentology and Sedimentary Basins: From Turbulence to Tectonics (2nd ed.): Wiley-Blackwell, West Sussex, UK, 63 p.

Legarreta, L., and, Uliana, M.A, 1994, Asociaciones de fósiles y hiatos en el Supracretácico-Neógeno de Patagonia: una perspectiva estratigráfico-secuencial: Ameghiniana, v. 31, p. 257–281.

Lesser, G., Roelvink, J., Van Kester, J., and Stelling, G., 2004, Development and validation of a three-dimensional morphological mode: Coastal Engineering, v. 51, p. 883–915.

Mack, G.H., James, W.C., and Monger, H.C., 1993, Classification of paleosols: Geological Society of America Bulletin, v. 105, p. 129–136.

Mastandrea, O., Leanza, H.A., Hugo, C.A., and Oblitas, C.J.J., 1983, Fosfatos sedimentarios marinos radioactivos en la Formación Salamanca (Terciario Inferior) Provincia del Chubut: Revista de la Asociación Geológica Argentina, v. 38, p. 185–191.

Malumián, N., and Caramés, A., 1995, El Daniano marino de Patagonia (Argentina): Paleobiogeografía de los foraminíferos bentónicos, *in* Náñez, C., ed., Paleógeno de América del Sur: Asociación Paleontológica Argentina Publicación Especial 3, Buenos Aires, p. 83–105.

Marciano, R., Wang, Z. B., Hibma, A., de Vriend, H. J., and Defina, A., 2005, Modeling of channel patterns in short tidal basins: Journal of Geophysical Research: Earth Surface, v. 110, doi: 10.1029/2003JF000092.

Marshall, L.G., Sempere, T., and Butler, R.F., 1997, Chronostratigraphy of the mammal-bearing Paleocene of South America: Journal of South American Earth Sciences, v. 10, p. 49–70.

Martínez, G.A., 1992, Paleoambiente de la Formación Salamanca en La Pampa María Santísima, Departamento Sarmiento, Provincia de Chubut: Revista de la Asociación Geológica Argentina, v. 47, p. 293–303.

Matheos, S.D., Brea, M., Ganuza, D., and Zamuner, A., 2001, Sedimentología y paleoecología del Terciario Inferior en el sur de la Provincia del Chubut, República Argentina: Revista de la Asociación Argentina de Sedimentología, v. 8, p. 93–104.

Matheos, S.D., Brea, M., Zucol, A.F., Prámparo, M., Raigemborn, M.S., Iglesias, A., and Fischer, A., 2005, Analisis paleoambiental de las sedimentitas del Daniano del sector sur de los Lagos Musters y Colhue Huapi (Chubut, Argentina): Actas XVI Congreso Geológico Argentino (La Plata), v. 3, p. 83–90.

Méndez, I., 1966, Foraminiferos, edad y correlaciones estratigráficas del Salamanquense de Punta Peligro (45x30'S; 67x11'W), provincia del Chubut: Revista de la Asociación Geológica Argentina, v. 21, p. 127–157.

Nouidar, M., and Chellai, E.H., 2001, Facies and sequence stratigraphy of an estuarine incised-valley fill: Lower Aptian Bouzergoun Formation, Agadir Basin, Morocco: Cretaceous Research, v. 22, p. 93–104.

Odin, G. S., and Fullagar, P.D., 1988, Geological significance of the glaucony facies: Developments in Sedimentology, v. 45, p. 295–332.

Pascual, R., Archer, M., Ortiz-Jaureguizar, E., Prado, J.L., Godthelp, H., and Hand, S.J., 1992, First discovery of monotremes in South America: Nature, v. 356, p. 704–706.

Pascual, R., Goin, F.J., Balarino, L., and Udrizar Sauthier, D.E., 2002, New data on the Paleocene monotreme *Monotrematum sudamericanum*, and the convergent evolution of triangulate molars: Acta Palaeontologica Polonica, v. 47, p. 487–492.

Petriella, B., and Archangelsky, S., 1975, Vegetación y ambiente en el Paleoceno de Chubut: Actas I Congreso Argentino de Paleontología y Bioestratigrafía, Tucumán, v. 2, p. 257–270.

Poppe, L., Paskevich, V., Hathaway, J., and Blackwood, D., 2001, A laboratory manual for X-ray powder diffraction: U.S. Geological Survey Open-File Report 01-041, 88 p.

Raigemborn, M., 2006, Analisis composicional y procedencia de la Formación Peñas Coloradas, Grupo Río Chico (Paleoceno Superior-Eoceno?), en la región oriental de la Cuenca del Golfo San Jorge, Chubut, Argentina: Latin American Journal of Sedimentology and Basin Analysis, v. 13, p. 65–87.

Raigemborn, M., Brea, M., Zucol, A., and Matheos, S., 2009, Early Paleogene climate at mid latitude in South America: Mineralogical and paleobotanical proxies from continental sequences in Golfo San Jorge basin (Patagonia, Argentina): Geologica Acta, v. 7, p. 125–145.

Raigemborn, María Sol, Gómez-Peral, L.E., Krause, J.M., and Matheos, S.D., 2014, Controls on clay mineral assemblages in an Early Paleogene nonmarine succession: Implications for the volcanic and paleoclimatic record of extra-Andean Patagonia, Argentina: Journal of South American Earth Sciences, v. 52, p. 1–23.

Rodriguez, J.F.R., and Littke, R., 2001, Petroleum generation and accumulation in the Golfo San Jorge Basin, Argentina: a basin modeling study: Marine and Petroleum Geology, v. 18, p. 995–1028.

Romero, E.J., 1968, *Palmoxylon patagonicum* n. sp. del Terciario Inferior de la Provincia de Chubut, Argentina: Ameghiniana, v. 5, p. 417–432.

Scafati, L., Melendé, D.L., and Wolkheimer, W., 2009, A Danian subtropical lacustrine palynobiota from South America (Bororó Formation, San Jorge Basin, Patagonia, Argentina): Geologica Acta, v. 7, p. 35–61.

Shanmugam, G., Poffenberger, M., and Alava, J.T., 2000, Tide-dominated estuarine facies in the Hollin and Napo ("T" and "U") formations (Cretaceous), Sacha field, Oriente basin, Ecuador: AAPG Bulletin, v. 84, p. 652–682.

Shieber, J., 1988, Storm sands with swaley cross-stratification in the lower Miocene Talião Formation, Taiwan: Neues Jahrbuch für Geologie und Paläontologie, v. 12, p. 718–734.

Singer, A., 1980, The paleoclimatic interpretation of clay minerals in soils and weathering profiles: Earth Science Reviews, v. 15, p. 303–326.

Spalletti, L.A., and Franzese, J.R., 2007, Mesozoic paleogeography and paleoenvironmental evolution of Patagonia (southern South America), *in* Gasparini, Z., Salgado, L., Coria, R.A., eds., Patagonian Mesozoic Reptiles, Bloomington: Indiana University Press, p. 29–49.

Sterli, J., and de la Fuente, M.S., 2012, New evidence from the Palaeocene of Patagonia (Argentina) on the evolution and palaeo-biogeography of Meiolaniformes (Testudinata, new taxon name): Journal of Systematic Palaeontology, v. 11, p. 835–852.

Sylwan, C., 2001, Geology of the Golfo San Jorge Basin, Argentina: Journal of Iberian Geology, v. 27, p. 123–157.

Tambussi, C. P., and Degrange, F.J., 2013, The Paleogene birds of South America, *in* Tambussi, C.P., and Degrange,F.J., eds., South American and Antarctic Continental Cenozoic Birds, Springer, Dordrecht, p. 29–47.

Tape, C. H., Cowan, C. A., and Runkel, A.C., 2003, Tidal-bundle sequences in the Jordan Sandstone (Upper Cambrian), southeastern Minnesota, USA: evidence for tides along inboard shorelines of the Sauk epicontinental sea: Journal of Sedimentary Research, v. 73, p. 354–366.

Uliana, M. A., and Biddle, C. A., 1988, Mesozoic–Cenozoic paleogeographic and geodynamic evolution of southern South America: Revista de la Asociación Geológica Argentina, v. 18, p. 172–190.

Umazano, A. M., Bellosi, E.S., Visconti, G., Jalfin, G.A., and Melchor, R.N., 2009, Sedimentary record of a Late Cretaceous volcanic arc in central Patagonia: petrography, geochemistry and provenance of fluvial volcaniclastic deposits of the Bajo Barreal Formation, San Jorge Basin, Argentina: Cretaceous Research, v. 30, p. 749–766.

van Maren, D.S., 2005, Barrier formation on an actively prograding delta system; the Red River Delta, Vietnam: Marine Geology, v. 224, p. 123–143.

White, P.D., and Schiebout, J., 2008, Paleogene paleosols and changes in pedogenesis during the initial Eocene thermal maximum: Big Bend National Park, Texas, USA: Geological Society of America Bulletin, v, 120, p. 1347–1361.

Wilf, P., Cúneo, N.R., Escapa, I.H., Pol, D., and Woodburne, M.O., 2013, Splendid and seldom isolated: the paleobiogeography of Patagonia: Annual Review of Earth and Planetary Sciences, v. 41, p. 561–603.

Willis, B.J., and Tang, H., 2010, Three-dimensional connectivity of point-bar deposits: Journal of Sedimentary Research, v. 80, p. 440–454.

Zamaloa, M.C., and Andreis, R.R., 1995, Asociación palinológica del Paleoceno temprano (Formación Salamanca) en Ea. Laguna Manantiales, Santa Cruz, Argentina: Actas VI Congreso Argentino de Paleontología y Bioestratigrafía, Trelew, v. 1, p. 301–305.

Zhang, J.L., and Zhang, Z.J., 2008, Sedimentary facies of the Silurian tide-dominated paleo-estuary of the Tazhong area in the Tarim Basin: Petroleum Science, v. 5, p. 95–104.

Received 17 July 2014; accepted 31 May 2015.